Identification of Muscle Activation at Rest

Author:

Áróra Helgadóttir
Student Number: 4182855
Submission Date: 01.07.2013

Graduation Committee:

Dr. ir. Alfred C. Schouten	BMechE, 3mE, TU Delft
Dr. ir. Erwin de Vlugt	BMechE, 3mE, TU Delft
Dr. ir. Jurriaan de Groot	Rehabilitation, LUMC
Dr. Jochem Nagels	Orthopedics, LUMC
Dr. rer. nat. Stephan G. Lukosch	TBM, TU Delft

Acknowledgements to my supervisor Dr. ir. Erwin de Vlugt and the supporting staff, Dr. ir. Jurriaan de Groot, Ir. Karin de Gooijer and Dr. Carel Meskers. I also want to thank the EXPLICIT group for the access to the data of the EXPLICIT study.

Abstract

Offset muscle activation is the constant neural firing to muscles, even at rest, defining the minimum muscle contraction. Until now, the offset muscle activation has been neglected in the analysis of the dynamical behavior of joints. There is a clinical need for an assessment method to estimate the contribution of the offset muscle activation to the total joint torque in stroke patients, in order to choose the optimum treatment method.

The goal of this study was to develop a method that estimates the offset muscle activation of the wrist joint muscles in vivo, in addition to other contributions from tissue viscoelasticity and stretch reflexes. For this purpose, an existing one-sided neuromuscular model of the ankle was extended to a two-sided wrist model for full biomechanical characterization over the whole range of flexion-extension movement. The model parameters (including offset activation, amongst others) were estimated from measured wrist torque, angle and EMG as recorded during imposed ramp-and-hold flexion and extension rotation.

It was found that offset muscle activation was present at rest, in both stroke patients and healthy controls. Both offset activity of the extensor carpi radialis (ECR) and reflex activity of the flexor carpi radialis (FCR) were increased in stroke patients compared to controls. The viscoelastic behavior of the FCR was changed in patients compared to controls.

From the results of this study it was concluded that following stroke a constant muscle force can be applied by the ECR, which may act as a counterbalance to the altered tissue viscoelasticity and possible shortening of the FCR muscle (or vice versa). Apparently, a new antagonistic force balance had developed around the wrist joint in the stroke patients, having a structural origin on one side and an active (neural) origin on the opposite side. The results may be of importance for targeted treatment of the movement disorder, when choosing for casting, drug therapy or surgical intervention.

1. Background

Stroke is the second most common cause of death in the world and is a leading cause of disability (Belda-Lois et al., 2011; Di Carlo, 2009), with 16 million new stroke incidents annually and 5.7 million deaths. About half of the survivors have a physical or cognitive disability (Di Carlo, 2009). The major causes of the abnormal function in upper limb are contracture and spasticity (Twitchell, 1951) but in fact the movement disorder following stroke is a complex interaction between the muscles, connective tissues and neural activation (Meskers et al., 2009). In different combinations the changes in neural and non-neural parts of the musculoskeletal system lead to an increased joint stiffness (Dietz & Sinkjaer, 2007; Lieber et al., 2004).

Contracture, defined as extremely stiff muscles, a loss of passive range of motion (ROM) and chronically deformed joint position (Kwah et al., 2012; Latash & Anson, 1996; Smith et al., 2011), is commonly observed in the wrist joint following stroke. This leads to a lack of hand control and function (Lannin et al., 2007). Contracture can occur following prolonged hyper activation of the muscle, such as spasticity (Smith et al., 2011) or hypertonia (Dietz & Sinkjaer, 2007; Latash & Anson, 1996). Recent studies have also related changes in tendons, collagen tissues and structural changes in muscle tissue to the joint contracture (Dietz & Sinkjaer, 2007).

Thus, it is clear that there can be different causes of the increased wrist stiffness and deformed position following stroke, both of neural and non-neural origins (Dietz & Sinkjaer, 2007; Lieber et al., 2004). The neural part in the joint stiffness originates from the reflexive response to stretch (de Vlugt et al., 2010; Mirbagheri et al., 2005; Sinkjaer & Magnussen, 1994; Thajchayapong et al., 2006). In addition, increased minimum muscle activation can contribute to abnormal neural activation of the muscles, as observed in stroke patients in the study of Burne et al. (2005) and referred to here as 'offset muscle activation'. The non-neural properties of passive tissues represent the stiffness and viscosity of the muscles and connective tissues. Due to the contribution from the nervous system and the muscular system it is important to study both parts in order to fully understand the pathophysiology of the movement disorder (de Vlugt et al., 2010; Lieber et al., 2004).

The applicability of a treatment method depends on the origin of the movement disorder of each patient. Treatments aiming at offset muscle activation or hyperactive reflexes can be pharmacological, such as Botulinum Toxin-A injections or baclofen ingestion (Logan, 2011; Sommerfeld et al., 2012). Treatments aiming at the increased tissue viscoelasticity are e.g. soft-tissue surgery and joint stabilization with splinting and casting (Logan, 2011; Renzenbrink et al., 2012). One of the most widely used clinical assessments of spasticity, and the movement disorder following stroke, is the Ashworth score (AS) and the modified Ashworth score (MAS) (Dietz & Sinkjaer, 2007). The examiner rotates the joint in a passive movement over the full range of motion in one second and subjectively grades the mechanical resistance sensed (Ashworth, 1964). The Ashworth score is mainly used to measure the severity of the spasticity of the patient and does not give any information about the underlying pathophysiology. There is no method available that fully separates the increased joint stiffness into the underlying contributors from the neural and non-neural origins.

Previous studies have separated neural and non-neural parts contributing to the total joint torque. Typically, tissue viscoelasticity and active muscle force were estimated from measured joint angle, torque and EMG signals (de Vlugt et al., 2010; Hof & Vandenberg, 1981; Lloyd & Besier, 2003). However, any offset muscle activation was ignored in all previous models, which means that torque from any offset muscle activation was obviously present in the measured joint torque but was disregarded from the EMG signals. As a consequence, any offset activation was likely attributed erroneously to other torque contributing components within the model being used, causing overestimation of e.g. passive viscoelasticity or reflexive torque, which might lead to improper treatment choice. In the study of Burne et al. (2005) the offset muscle activation of patients and controls was matched with a new normalization method. With this method the hyper reflex activity and increased passive stiffness was not found in the patients, contrasting the case without normalization. The results showed that the patient had a smaller range of reflex modulation than normally, possibly due to the decreased maximum voluntary contraction (muscle weakness) and increased offset muscle activation. The difference in results when taking the offset activation into account emphasizes the importance of separating the offset part from the total joint torque, in order to be able to quantify the contribution of the offset activation in patients.

In some cases an improper treatment is applied, e.g. if hyperactive reflexes or increased offset muscle activation are wrongly assumed to be the cause of the movement disorder and a neural block is applied, only weakening the affected muscle without improving the condition of the patient (Logan, 2011; Meskers et al., 2009). Thus, in order to prevent making the patient's condition worse by applying inappropriate treatment it is important to know the main origin of the movement disorder.

The goal of this study was to extend a single agonist ankle model to a double-sided wrist model and separate the torque contribution of the offset muscle activation from the total joint torque during flexion and extension rotations. The key assumption made in this study was that the measured EMG signal consisted of three distinguishable parts, being: 1) a varying part related to stretch reflexes and voluntary control; 2) a constant offset muscle activation, and 3) a constant measurement noise not contributing to the muscle force. The hypothesis is that this key assumption will enable quantification of the contribution from the offset muscle activation to the total wrist torque in response to a stretch. Further, the new method will enable more reliable separation of the different parts contributing to the total joint mechanical behavior, namely the offset muscle activity, (hyperactive) reflexes and (increased) stiffness and viscosity of passive tissues. A nonlinear neuromuscular model will be developed and used to estimate these properties in both stroke patients and healthy subjects. The aim is to answer the following questions:

1. Can humans bring muscle activation to zero at rest, i.e. when instructed to be at rest?
2. Is muscle activation in resting state higher in stroke patients compared to healthy subjects?
3. Can muscle activity be reliably estimated from the joint mechanical response?

By succeeding this goal, the proposed method may provide clinicians a new and valuable tool for choosing the right treatment for each individual patient.

2. Methods

2.1. Database

The pilot database from the EXPLICIT study (EXPLICIT-stroke: Explaining Plasticity after Stroke, (Klomp et al., 2012; Kwakkel et al., 2008) was used, which enabled application of the model to a large amount of data that was readily available.

2.1.1. Patients & Controls

The pilot database contains measurements, from one or two visits, from 32 chronic stroke patients (mean age 58.5 years, SD 13.1) with modified Ashworth scores from 0 to 4, from the outpatient clinics of the Department of Rehabilitation Medicine of the Leiden University Medical Center and the Rijnland's Rehabilitation Center, Leiden, the Netherlands. The inclusion criteria were that the stroke occurred in the period from 1998 to 2008 and the patients were still experiencing some rest effects of the stroke in the arm, so fully recovered patients were excluded. The pilot database contains measurements from two or three visits of 14 healthy subjects (mean age 49.4, SD 15.1), used as a control group. The exclusion criteria for healthy subjects were no prior neurological deficiencies (J.M. van der Krogt, personal communication, 5.6.2013).

2.1.2. Instrumentation

The subjects were seated with their shoulder relaxed and elbow flexed in approximately 90°. Haptic wrist manipulator, the Wristalyzer® (Moog, Nieuw Vennep, the Netherlands) was used in the measurements, see Figure 1. The arm of the subject was attached to the device and the hand attached to a rotating handle with Velcro straps. The handle was rotated with a vertically positioned servo motor (Parker SMH100 series). The axis of rotation of the wrist was aligned with the axis of rotation of the motor, such that the rotation of the handle was directly related to the flexion and extension of the wrist. The ROM of the handle was approximately 180°, with accuracy of 0.35° (Klomp et al., 2012) and positive rotation was defined in wrist flexion and negative in the wrist extension. The motor was driven in two different ways, either by torque to measure the wrist range of motion (ROM) or by position in a ramp-and-hold (RaH) signal to rotate the wrist over the ROM. Further information about the measurement protocol can be found in subchapter 2.1.3.

The neural muscle activation was measured with Delsys Bagnoli-8 system (Delsys Inc., Boston, the USA) with bipolar surface electrodes. Two electrodes were placed on the flexor carpi radialis (FCR) and two on the extensor carpi radialis (ECR) (Klomp et al., 2012). The EMG signals were sampled at 2048 Hz and off-line rectified and integrated by low pass filtering (3rd order Butterworth) at 20 Hz (IEMG). The wrist torque and angle were sampled with the same frequency, 2048 Hz. The angular velocity and acceleration were derived by single and double integrating the angular position of the wrist. The joint angle and wrist torque were low pass filtered (3rd order Butterworth) at 20 Hz in order to prevent amplifying noise due to differentiation.

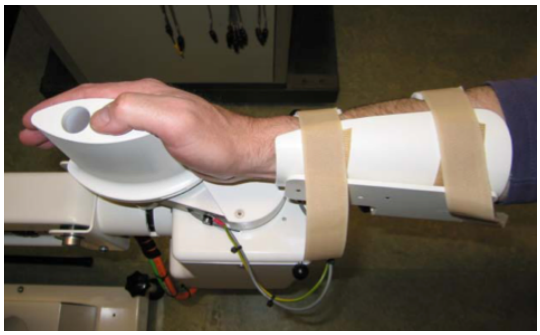

Figure 1: Experimental setup, top-view of the Wristalyzer® (Moog, Nieuw Vennep, the Netherlands). For clearer view of the configuration of the hand the fixation straps of the hand were not shown. From Klomp et al., 2012.

2.1.3. Protocol

The EXPLICIT protocol includes a variety of different tests, both passive and active, with both position and force tasks. Only a part of the protocol was applicable for this study and will be explained, which is the reflexive test ASH. Other tests performed during the experiment but not used for this study were passive range of motion (ROMP), stiffness in rest (SIR), active range of motion (ROMA), maximal voluntary contraction (MVC), control over joint torque (CJT) and neural looptime (NL). The total measuring time was approximately 45 minutes, including the instructions and practice but excluding the EMG placement (Klomp et al., 2012).

Ashworth - ASH

This is an automatic version of the clinical modified Ashworth score. The subject was asked to remain relaxed during the measurement. The wrist was rotated over full ROM of each subject with a ramp-and-hold (RaH) input signal with two different ramp durations, 1 second and 0.5 seconds. The wrist was rotated at a constant velocity, individually determined by the ROM of each subject and the ramp duration. Only 1-second ramp was applied to the control subjects of the pilot study. The EMG was measured during the RaH rotation. The test was applied twice and in the opposite directions, that is, the wrist was extended from fully flexed position, rotated to the neutral position and then flexed from fully extended position, or the other way around (Klomp et al., 2012). Therefore each measurement for certain RaH signal resulted in two data observations.

2.2. Neuromuscular Model and Parameter Estimation

A nonlinear neuromuscular computer model of the wrist joint was built to predict the torque response of the joint. The model was based on the single-sided ankle joint model from de Vlugt et al. (2010), but was adjusted to the wrist joint. In addition, in order to quantify the torque contribution from both the extensor muscles and the flexor muscles of the joint the model was made two-sided. The model comprised passive and active muscle elements representing flexor and extensor muscles of the wrist, that is, the FCR and the ECR. The tendons were assumed to be infinitely stiff. A mechanical representation of the model can be seen in Figure 2.

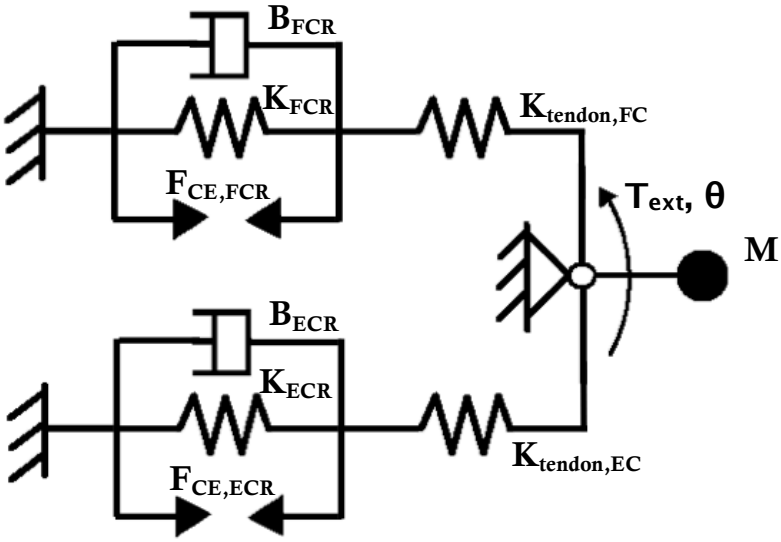

Figure 2: Mechanical representation of the neuromuscular model. M is the point mass of the hand and the rotating handle. The external torque, T_{ext}, and the angular position of the wrist, θ, are positive in flexion direction. The flexor muscle, FCR, is represented on top and the extensor muscle, ECR, below. Both muscles are represented with passive viscous element, passive stiffness element and contractile element. The tendons are assumed to be infinitely stiff.

The inputs of the wrist model were the measured joint angle and the IEMG and the output was the joint torque. The model was fitted onto the measured torque over a timeframe of 0.5 s before to 0.5 s after the imposed ramp rotation. A criterion function (error function) was defined to minimize the quadratic difference between the measured and modeled wrist torques by optimizing the free parameters. The error can be represented with:

$$e(t) = T_{meas}(t) - T_{mod}(t)$$

A flowchart of the method can be seen in Figure 3.

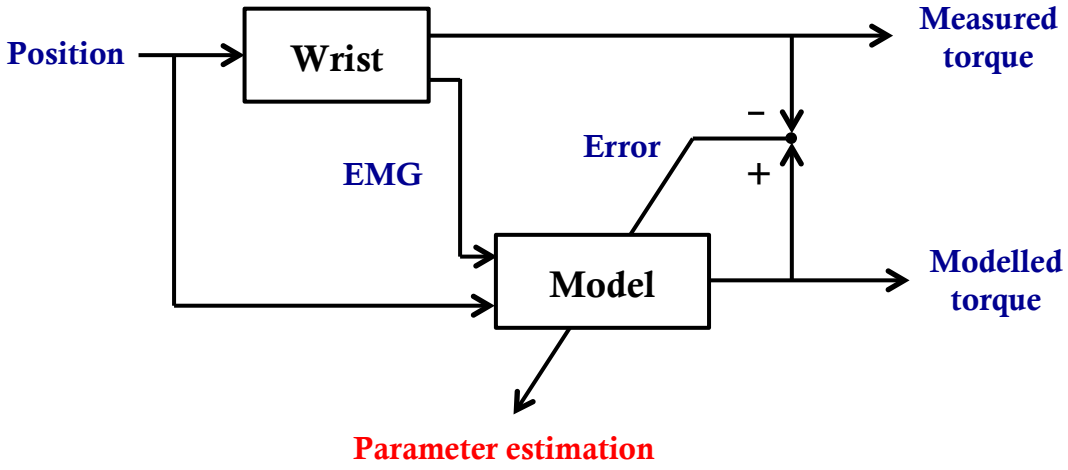

Figure 3: A flowchart of the method used in the study. The Wrist block represents the wrist of the subject and the Model block represents the model, used to predict the torque response of the subject. The inputs to the model are the measured position and EMG signal and the output is the modeled torque. The model minimizes the error between the measured and modeled torques with a criterion function, by optimizing the free parameters of the model (see Table 1).

The data from the two observations in opposite directions (flexion and extension) at the same measurement condition was optimized in one run, such that the same parameter values were used to model the torques in flexion rotation and extension rotation. The data analysis and parameter estimation was performed in MATLAB (The Mathworks Inc., Natick MA). In total 13 parameters were optimized, summarized in Table 1.

Table 1: Model parameters, description and the initial values used for optimization.

Parameter	Unit	Description	Initial Value
$\boldsymbol{m}$	kg	Mass (hand + handle)	0.75
$\boldsymbol{b_{ECR}}$	Ns/m	ECR viscosity coefficient	50
$\boldsymbol{b_{FCR}}$	Ns/m	FCR viscosity coefficient	40
$\boldsymbol{k_{ECR}}$	1/m	ECR stiffness coefficient	110
$\boldsymbol{k_{FCR}}$	1/m	FCR stiffness coefficient	130
$\boldsymbol{x_{0,ECR}}$	m	ECR muscle force shift	0.035
$\boldsymbol{x_{0,FCR}}$	m	FCR muscle force shift	0.032
$\boldsymbol{e_1, e_2, e_3, e_4}$	N/Volts	EMG weighting factors	$1{\cdot}10^3$
$\boldsymbol{c_{noise,ECR}}$	N	Noise in ECR EMG	350
$\boldsymbol{c_{noise,FCR}}$	N	Noise in FCR EMG	350

The wrist joint torque response was described with:

$$T_{mod}(t) = I\ddot{\theta}(t) + T_{FCR}(t) - T_{ECR}(t)$$

where t is the independent time variable [s]. T_{mod} is the modeled total torque from the wrist [Nm], T_{FCR} and T_{ECR} are the torque contributions from the FCR and ECR [Nm], respectively. I is the inertia of the hand and the handle [kg·m^2] and $\ddot{\theta}(t)$ is the angular acceleration of the wrist [rad/s^2].

The torque response from each muscle was modeled by taking into account the passive and active muscle properties:

$$T_{FCR}(t) = \left(F_{active,FCR}(t) + F_{visc,FCR}(x,\dot{x}) + F_{stiff,FCR}(x)\right) r_{FCR}(\theta)$$

$$T_{ECR}(t) = \left(F_{active,ECR}(t) + F_{visc,ECR}(x,\dot{x}) + F_{stiff,ECR}(x)\right) r_{ECR}(\theta)$$

where the passive ($F_{visc,FCR}$ and $F_{stiff,FCR}$) and active ($F_{active,FCR}$) muscle elements were identical in structure to those previously described by de Vlugt et al. (2010) as used for the triceps surae of the ankle.

The active part, $F_{active,FCR}(t)$, was modeled using Hill-type muscle model (see Appendix, equation A20). The neural muscle activity (input of the Hill-type muscle model) of both the FCR and the ECR was estimated from the IEMG signals from the measurements. In this study the IEMG signal was assumed to consist of three parts to be identified, shown in a schematic and simplified way in Figure 4. The first part is from reflexive responses to the imposed joint rotation and eventually from voluntary control. The second part is an involuntary constant drive, the offset excitation, determining the minimum muscle activation. The third part is from sources that are not correlated to the muscle force causing the wrist torque, e.g. from other muscles and measurement noise. The noise part was assumed to be constant throughout the observation.

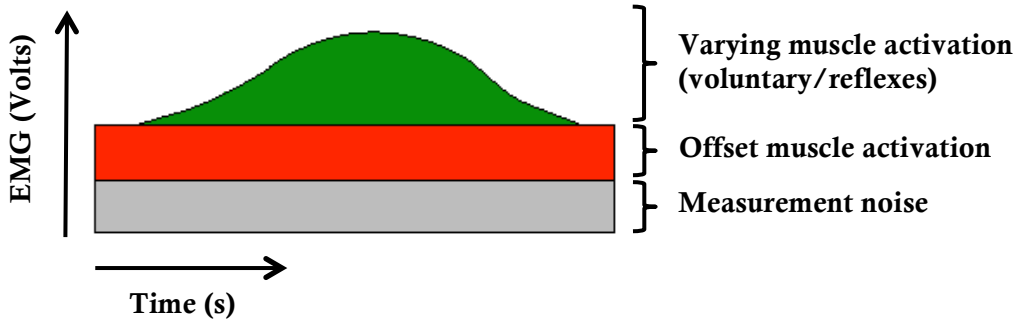

Figure 4: Assumption of the composition of the measured EMG signal; constant offset muscle activation, varying muscle activation from reflexes and voluntary input and a constant measurement noise.

Noise was modelled by $c_{noise,FCR}$ and $c_{noise,ECR}$ for the FCR and ECR IEMG signals respectively, and estimated from the parameter optimization procedure. After the parameter optimization the neural excitation that does correspond to the wrist torque (offset and varying excitation) was found by subtracting the noise portions from the corresponding IEMG:

$$u_{FCR} = e_1 IEMG_{FCR,dist}(t) + e_3 IEMG_{FCR,prox}(t) - c_{noise,FCR}$$

$$u_{ECR} = e_2 IEMG_{ECR,dist}(t) + e_4 IEMG_{ECR,prox}(t) - c_{noise,ECR}$$

where u_{FCR} and u_{ECR} are the modeled neural muscle excitations of the flexor carpi radialis and the extensor carpi radialis respectively, $e_1 - e_4$ are optimized weighting factors [N/V] to estimate the offset and varying excitations and the different IEMG terms correspond to the electrodes placed distally and proximally on each muscle. The estimated excitation signals, u_{FCR} and u_{ECR}, represent the true muscle excitation (offset and varying excitation).

Offset excitation, $u_{FCR,offset}$, was taken as the minimum value of the total neural excitation, u_{FCR}, (average over a subsequent windows of 0.167 s). The estimated excitation signals, u_{FCR} and $u_{FCR,offset}$, were fed to the modelled muscle activation dynamics to find the resulting muscle activation (Appendix, equation A19). The same was done for the ECR. Finally, the active muscle force was derived from simulation of the Hill-type muscle model by using the synthesized muscle activation and the recorded joint rotation (see Appendix, equation A20 and A21). The muscle force from the varying muscle activation was

derived by subtracting the muscle force corresponding to the offset activation from the total active muscle force (see Appendix, equation A22).

The passive parts, $F_{visc,FCR}(x, \dot{x})$ and $F_{stiff,FCR}(x)$, were modeled using the exponential force-length and force-velocity relationships:

$$F_{visc,FCR}(t) = e^{k_{FCR}(x_{FCR}(t)-x_{0,FCR})}\dot{x}_{FCR}(t)b_{FCR}$$

$$F_{stiff,FCR}(t) = e^{k_{FCR}(x_{FCR}(t)-x_{0,FCR})}$$

and the same for the ECR. Both the viscous and stiffness force depends on the wrist position, with an exponential relation. The amount of viscous force is defined by the viscosity coefficient b [Ns/m] and the shape of the exponential stiffness curve is defined by k [1/m]. In order to enable a shift in the viscous and stiffness forces a shift parameter, x_0 [m], is included. It determines at what muscle length the force starts increasing exponentially.

The initial values of the non-neural parameters (b_{ECR}, b_{FCR}, k_{ECR}, k_{FCR}, $x_{0,ECR}$ and $x_{0,FCR}$) were chosen by simulating hysteresis cycle (the viscous behavior, not relaxation and creep), by applying triangular input rotation to the passive part of the model and plotting the simulated torque response. The rotation applied to the model equaled the average ROM of the control subjects of this study (approximately -55° to 85°). The initial values were changed (trial and error) until the torque response was similar to what was found in literature (see Figure 3 in Klomp et al, 2011). This resulted in slightly different initial values of the corresponding parameters of the FCR and the ECR. The initial values of the neural parameters ($e_1, e_2, e_3, e_4, c_{noise,FCR}$ and $c_{noise,ECR}$) were chosen by applying the model to measured data and changing the values (trial and error) until acceptable model fits were derived.

For analysis both the offset excitation and the varying excitation were presented by their corresponding joint torques as root mean squares (r.m.s.) over the optimized time period (see Appendix, equation A23).

The passive tissue properties, stiffness and viscosity, were analysed in two different ways, with one-point analysis and by looking into the optimized parameter values. The passive stiffness and viscosity of the joint increase exponentially with joint angle and in previous studies a certain angle has been chosen in order to compare the estimated values between subjects. This one-point analysis was also used in this study in order to compare the results to literature. Since the model was two-sided two angles were chosen, $\theta_{comp,flex}$ and $\theta_{comp,ext}$. The average maximum flexion and extension angles of the control subjects (85° and -55°) were chosen for inter-subject analysis of passive tissue stiffness and viscosity, expected to show the largest contrast between subjects. The equations used to calculate the stiffness and the viscosity of the joint at $\theta_{comp,flex}$ and $\theta_{comp,ext}$ can be found in Appendix, A13 to A16. In literature, the angle 0° is most frequently used for estimation of the dynamic properties of the wrist joint (De Serres & Milner, 1991; Gielen & Houk, 1984; Rijnveld & Krebs, 2007) and was therefore chosen for model validation. To see the overall behavior of the passive tissues the full stiffness torque curves was plotted. The steepness of the curves is described with the optimized stiffness coefficient, k, and the start of the exponential increase in torque is described with the optimized muscle force shift, x_0. The viscous torque does not contribute much to the total torque and will not

be analysed in detail, but the optimized viscosity coefficient, *b,* indicates the amount of velocity dependence of the tissues.

2.3. Model Verification

For verification of the model two different measures were used. Firstly, the covariance matrix P was derived with:

$$P = \frac{1}{N} \cdot (J^T \cdot J)^{-1} e \cdot e^T$$

where N is the number of time samples used for the parameter optimization, J is the Jacobian matrix and e is the $1 \times N$ error vector. The Jacobian is a $N \times n_p$ matrix where $n_p = 13$ is the number of optimized parameters and it contains the first derivatives of the final error to each parameter. The square root of the auto-covariance, the diagonal terms of P, is the standard error of mean (SEM). The SEM values were used to estimate the sensitivity of the parameters, but SEM is an indication how sensitive each parameter is with respect to the error function. A higher SEM value means the corresponding parameter is less reliable.
Secondly, the internal validity of the model was estimated with the Variance Accounted For (VAF), which indicates how well the model was able to predict the measured torque:

$$VAF = \left(1 - \frac{\sum(T_{meas}(t) - T_{mod}(t))^2}{\sum(T_{meas}(t))^2}\right) \cdot 100\%$$

where $T_{meas}(t)$ is the measured wrist torque and $T_{mod}(t)$ is the modelled torque over the time interval chosen for parameter optimization. Two different VAF values were derived for each optimization, one for the extension observation and one for the flexion observation.

2.4. Method Validation

Forward simulation was used to validate the method, that is, one measurement was used for parameter estimation and the optimized parameters were used to forward simulate the torque response of a different measurement. By using the optimized parameters to model the torque response at a different measurement condition, it comes clear if the model has captured the general behavior of the system and not only the behavior in the optimized condition. Two different validation conditions were used; different input signals and different subject visits. In the first validation condition the input signal was changed during the same visit, so the parameters were optimized for the response to a 0.5 s RaH rotation and all the parameters were kept fixed to forward simulate the wrist response to a 1 s RaH rotation. In the second validation condition 1 s RaH rotation was used for both optimization and forward simulation but the data was collected in two different visits. Due to the possibility of slightly changed EMG electrode position in the second visit, causing different scaling and measurement noise of the measured EMG signal, the parameters for the neural part ($e_1, e_2, e_3\ e_4, c_{noise,ECR}$, $c_{noise,FCR}$) of the wrist dynamics were left free and optimized again in the forward simulation. The parameters of the non-neural part of the system were kept fixed.

The Variance Accounted For (VAF) was used to estimate the goodness of the fit of the forward simulated torque responses.

2.5. Statistical Analysis

To compare the results between the patients and controls (the torque from offset muscle activation (r.m.s.), the torque from reflexive response (r.m.s.), the passive stiffness, passive viscosity and parameter values) a nonparametric Mann-Whitney U test was used, with alpha of 0.05. All statistical testing was performed using SPSS 20.0 (SPSS Inc., Chicago, USA).

3. Results

An overview of the number of observations used for parameter estimation and method validation with forward simulation, and number of discarded observations, can be found in Table 2. For data analysis all results from 1 s RaH measurements from all visits of both patients and control subjects were used for parameter estimation, except for the ones discarded due to measurement errors (explained in next paragraph). There were in total 114 observations of patients and 66 of controls. For model validation with forward simulation of different RaH rotations the number of observations was 92 for patients and 0 for controls (no 0.5 second RaH data available for controls in EXPLICIT pilot data). In order to use a patient for the RaH forward simulation there needed to exist data from both 1 s and 0.5 s RaH rotations, measured in the same visit, and such combinations were used from all visits of all patients. For model validation with forward simulation of 2nd visits the number of observations was 45 for patients and 24 for controls. In order to use a subject for the 2nd visit forward simulation there needed to exist data from 1 s RaH rotations from two different visits.

In two observations, from two patients, the hold phase after the ramp was not stable and showed unexpected oscillating rotations. These observations were discarded since they were not in agreement with the design of the measurement. Since both the flexion and extension observations are needed for model optimization the observation of the opposite direction could not be used either. Thus, for one patient two observations of 1 s RaH rotation were discarded and for the other patients two observations of 0.5 s RaH rotation were discarded. Two observations from 1 s RaH rotation of one control subject were discarded due to abnormal torque response, possibly caused by poor fixation of the hand to the rotating handle.

In 10 observations, from three patients, only 1 s RaH was applied so the data from these visits were not possible to use for forward simulation of 1 s RaH rotation. Five patients and one control subject only visited once or only data from one visit was available (2nd visit discarded due to previously explained reasons) and could therefore not be used for forward simulation of the 2nd visit. Six control subjects visited three times and results from all three visits were used for data analysis to enrich the data. For forward simulation of the 2nd visit only the first two visits of these subjects were used. The reasons for discarded data in the forward simulations can be found in subchapter 3.3.

Table 2: Overview of number of observations used for parameter estimation (data analysis), forward simulation and number of observations discarded from analysis.

		Number of observations used (available)		Number of observations discarded	
		Patients	**Controls**	**Patients**	**Controls**
Parameter Estimation		114 (116)	66 (68)	2	2
Forward Simulation (prediction)	**2nd visit**	44 (52)	24 (26)	8	2
	Different RaH	91 (106)	0 (0)	15	0

3.1. Torque Response and Model Output

The optimized parameter values of patients and controls (mean ± 1 s.d.) can be seen in Table 3. In Figure 5 examples of the model fits and the measured torque responses are shown. Figure 5 shows the extension rotation of the wrist during one second RaH rotation of one patient and one control subject. In Figure 5: A and B, the measured joint position can be seen, from full flexion to full extension. In Figure 5: C and D, the measured and the modeled torques from the wrist can be seen. The viscous and stiffness torques from the passive connective tissues can be seen in Figure 5: E and F. The total active muscle torques from the ECR and the FCR can be seen in Figure 5: G and H. The stiffness torque increases fast after onset of the rotation and reaches maximum at the hold phase. The viscosity contributes less to the total torque than the stiffness. The active muscle torque is much higher for the patient than the control subject and peaks around the end of the ramp at fully extended position.

Table 3: Model parameters, initial values used for optimization and the optimized values (mean and standard deviation of all visits of all subjects at 1 s RaH rotation).

Parameter	Unit	Initial Value	Estimated Value (mean ± 1 s.d.)
$\boldsymbol{m}$	kg	0.75	0.668 ± 0.233
$\boldsymbol{b_{ECR}}$	Ns/m	50	76.4± 76.5
$\boldsymbol{b_{FCR}}$	Ns/m	40	23.0 ± 25.8
$\boldsymbol{k_{ECR}}$	1/m	110	447± 190
$\boldsymbol{k_{FCR}}$	1/m	130	334 ± 120
$\boldsymbol{x_{0,ECR}}$	m	0.035	0.0711 ± 0.0104
$\boldsymbol{x_{0,FCR}}$	m	0.032	0.0522 ± 0.0195
$\boldsymbol{e_1, e_2, e_3, e_4}$	N/Volts	$1 \cdot 10^3$	2.05 ± 5.48, 0.748 ± 2.35, 1.33 ± 2.55, 1.25 ± 2.42 ($\times 10^4$)
$\boldsymbol{c_{noise,ECR}}$	N	350	385 ± 347
$\boldsymbol{c_{noise,FCR}}$	N	350	257 ± 285

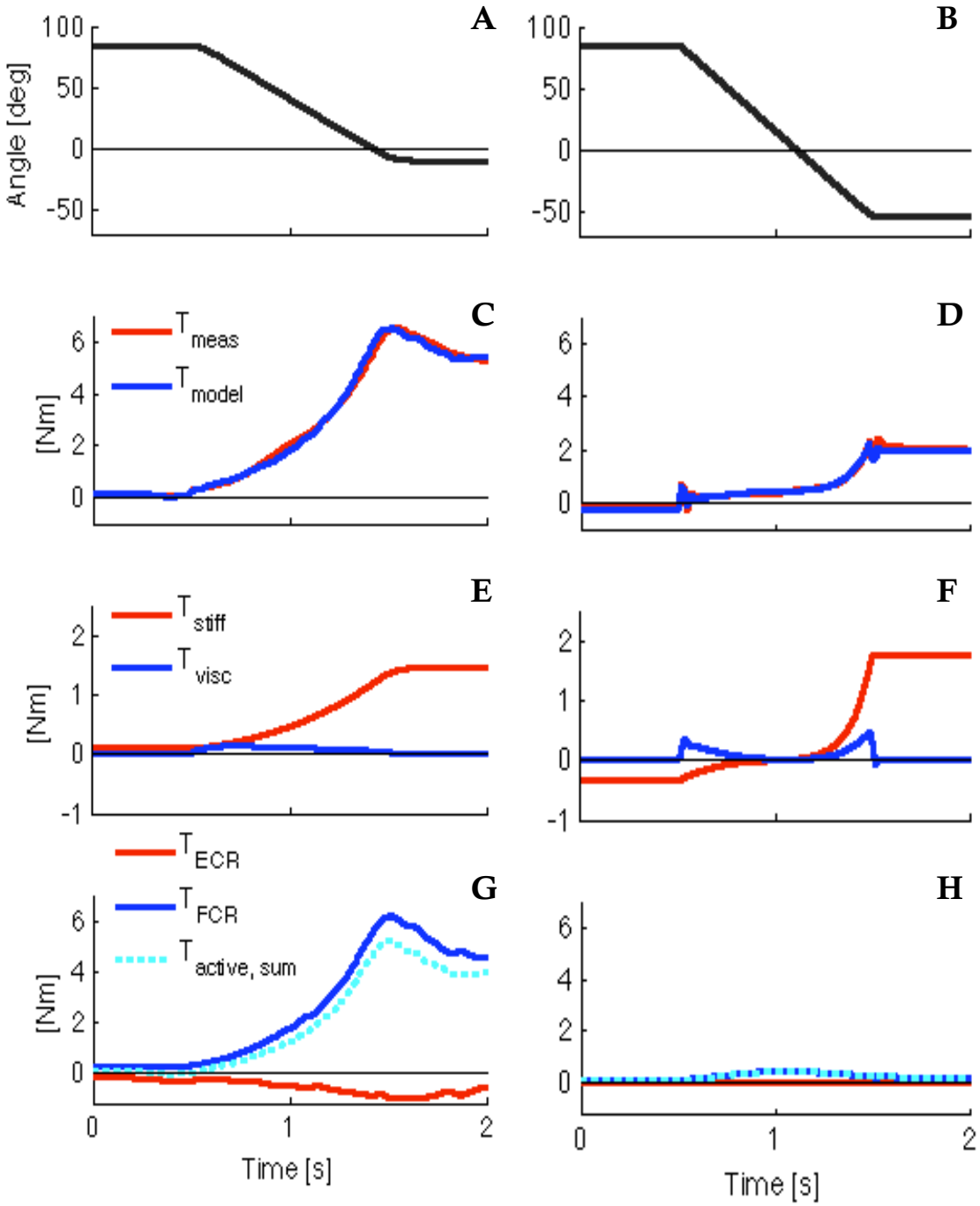

Figure 5: Model fits at 1 s RaH extension rotation over full ROM of each subject. Left column is patient data and right column is control data. A-B: imposed wrist movement; C-D: measured wrist torque (red) and predicted torque from muscle activity of ECR (red), FCR (blue) and total (dotted light blue).

Figure 6 shows the same as Figure 5 but for flexion rotation, so from full extension to full flexion. The same principles can be seen as in the previous figure except that in the starting position, at full extension, the muscle activity is the highest.

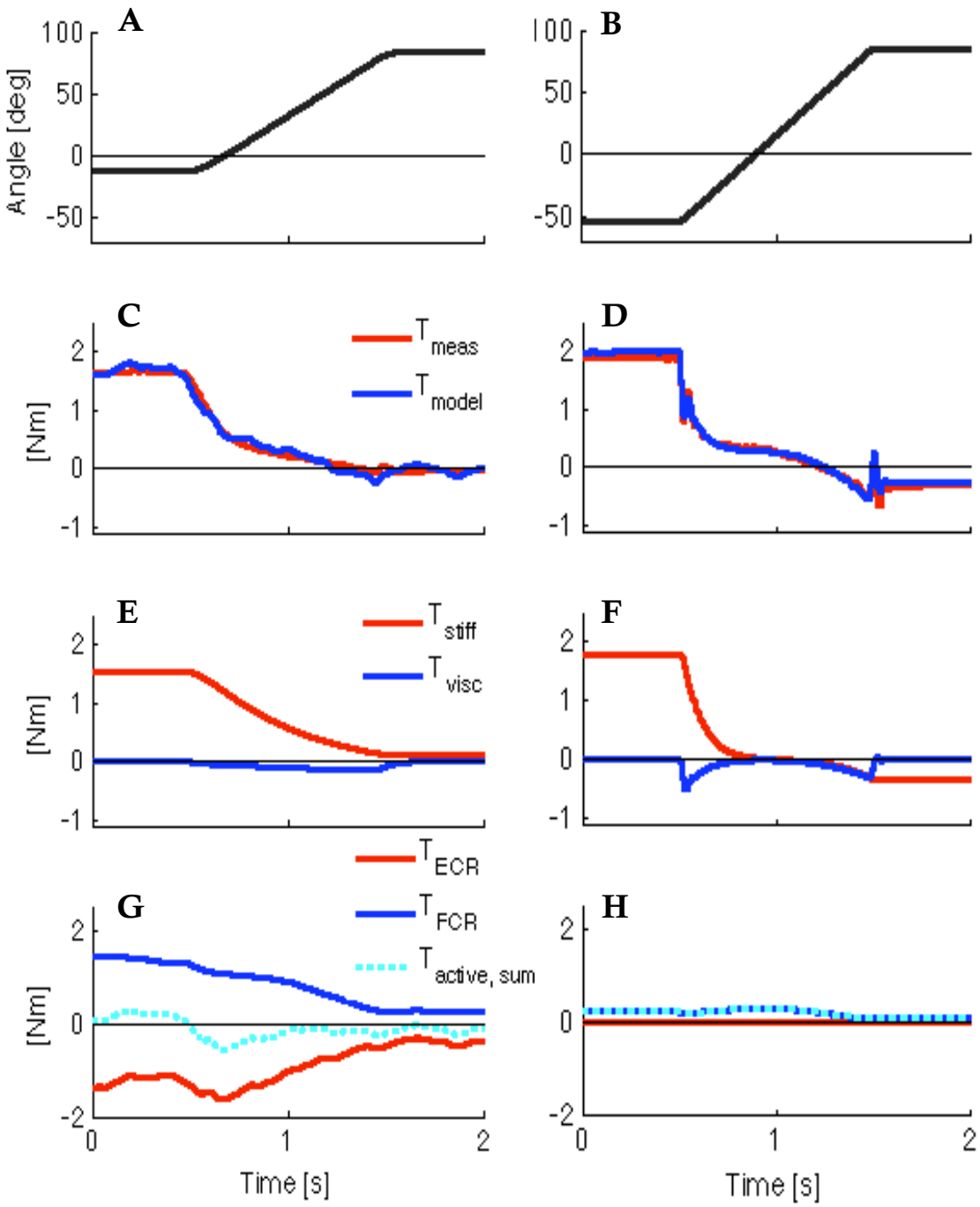

Figure 6: Model fits at 1 s RaH flexion rotation over full ROM of each subject. Left column is patient data and right column is control data. A-B: imposed wrist movement; C-D: measured wrist torque (red) and predicted torque from model (blue); E-F: torque from stiffness (red) and viscosity (blue) of passive tissues; G-H: torque from muscle activity of ECR (red), FCR (blue) and total (dotted light blue).

More detailed representation of the active muscle torque of the patient can be seen in Figure 7, where the offset muscle torque has been separated from the total active muscle torque. In Figure 7: A and B, the direction of the rotation and the onset of the rotation can be seen. The separated torque contributions from total active muscle activation and the offset muscle activation can be seen in Figure 7: C and D. The modeled EMG activity of the two muscles can be seen in Figure 7: E and F, where the estimated offset muscle activation is also shown. The torque contributions from FCR offset muscle activation are similar for both directions, but the torque due to the ECR offset muscle activation is higher for the flexion

than the extension rotation. The contribution of FCR reflexive torque is large in extension, when the muscle is being stretched, but smaller in the flexion when the tension on the muscle is released. Similar behavior can be seen for the ECR, where the contribution from the reflexive torque is larger in flexion than in extension rotation. The shape of the torque curves from the offset muscle activation shows the behavior of an elongating active muscle, so the shape of this curve is partly related to the force-length relationship of active muscles.

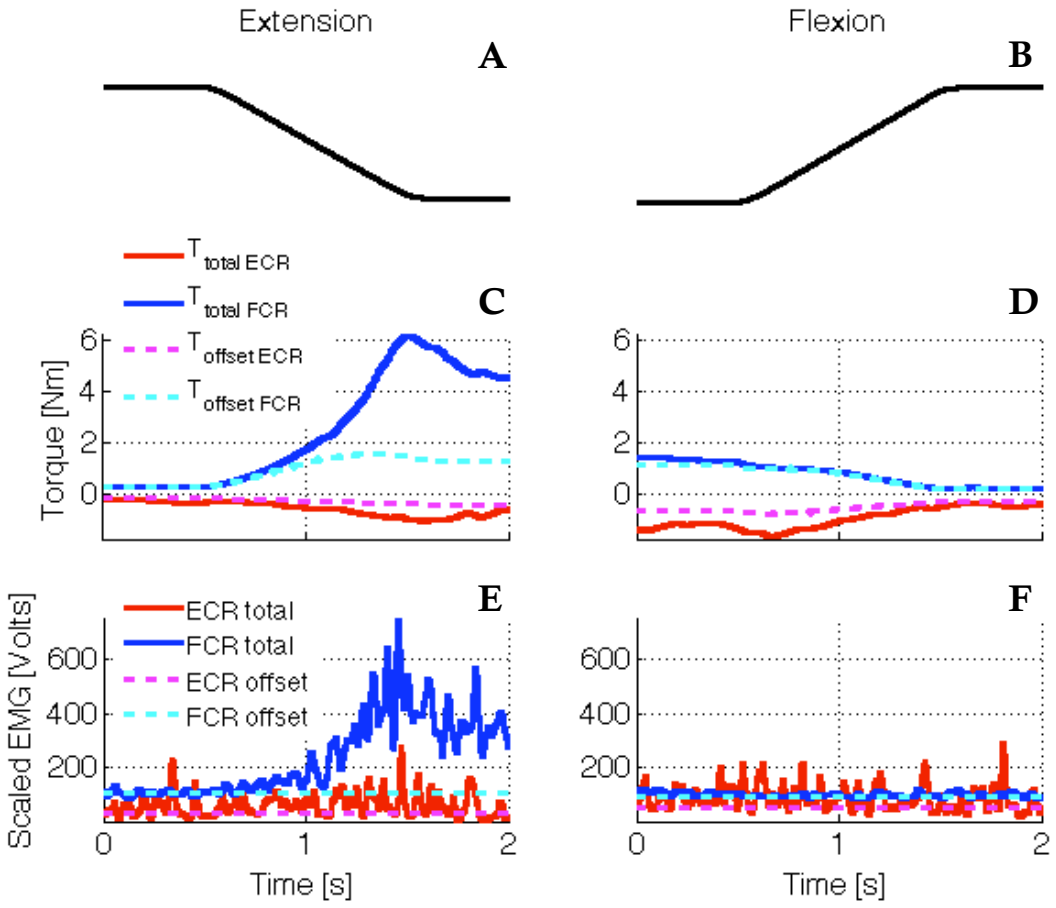

Figure 7: Active muscle torque response for the same patient. Left column shows the extension rotation and the right column shows the flexion rotation. A-B: imposed wrist movement; C-D: torque from total muscle activity of ECR (red), FCR (blue), torque from ECR offset (dotted pink) and torque from FCR offset (dotted light blue); E-F: scaled IEMG signal, total from ECR (red), total from FCR (blue), ECR offset (dotted pink) and FCR offset (dotted light blue).

Figure 8 shows the same as Figure 7, but for the control subject. In this case there is no contribution from ECR active muscle torque to the total wrist torque. There is a contribution from the FCR offset torque, similar for both directions. No FCR reflex torque is seen in the extension rotation but a slight reflexive response is seen in the flexion rotation.

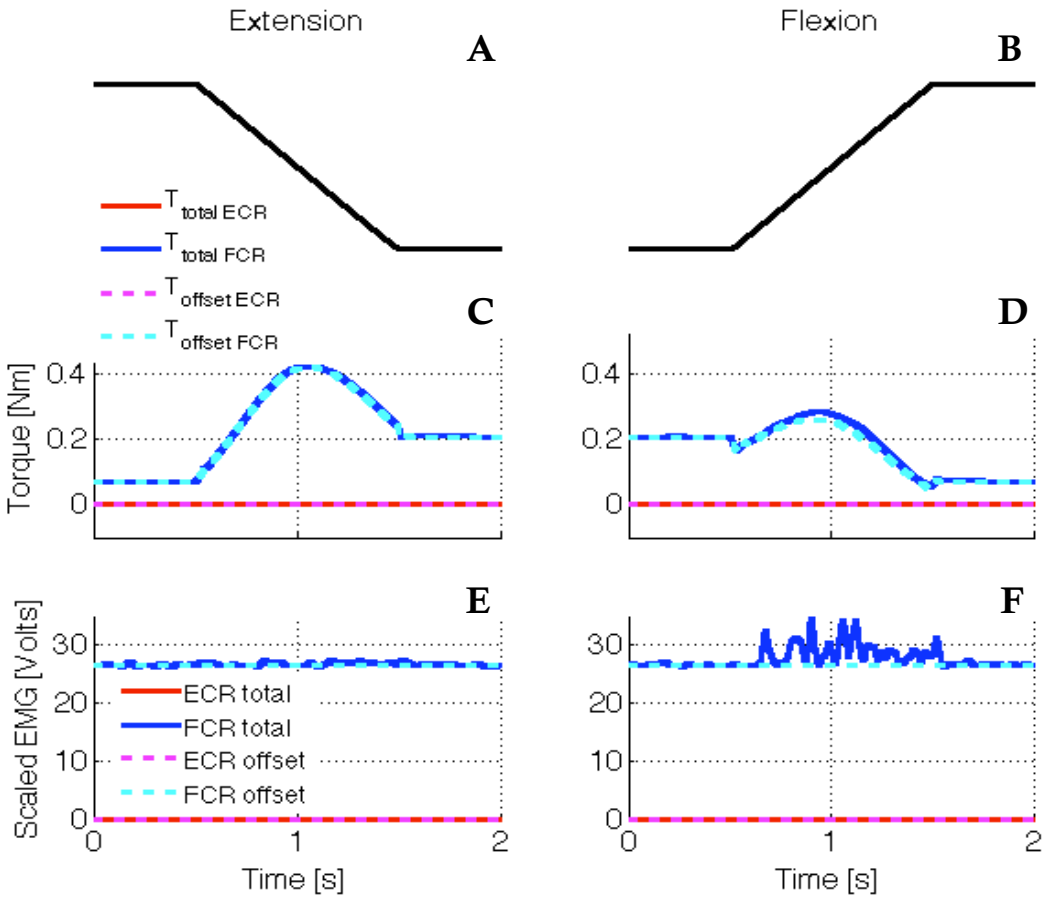

Figure 8: Active muscle torque response for the same control subject. Left column shows the extension rotation and the right column shows the flexion rotation. A-B: imposed wrist movement; C-D: torque from total muscle activity of ECR (red), FCR (blue), torque from ECR offset (dotted pink) and torque from FCR offset (dotted light blue); E-F: scaled IEMG signal, total from ECR (red), total from FCR (blue), ECR offset (dotted pink) and FCR offset (dotted light blue).

3.2. Model Validity & Parameter Accuracy

For all measured data with 1 s RaH rotation the Variance Accounted For (VAF) was above 87%, but above 95% in 174 observations of total 180. In total for the 180 observations the VAF was 98.4 ± 1.8 (mean ± 1 s.d.). This means that the model did represent the wrist torque response well in most cases, so the structure of the model is able to describe dynamical behavior of the wrist.

The SEM values of the optimized parameters for all model predictions for wrist torque response to 1 s RaH rotations for both patients and controls can be seen in Figure 9 and Figure 10. The 75th percentile of the SEM values for all parameters, except for the IEMG scaling factors, was below 0.15. The EMG weighting factors ($e_1 - e_4$) were the least sensitive parameters.

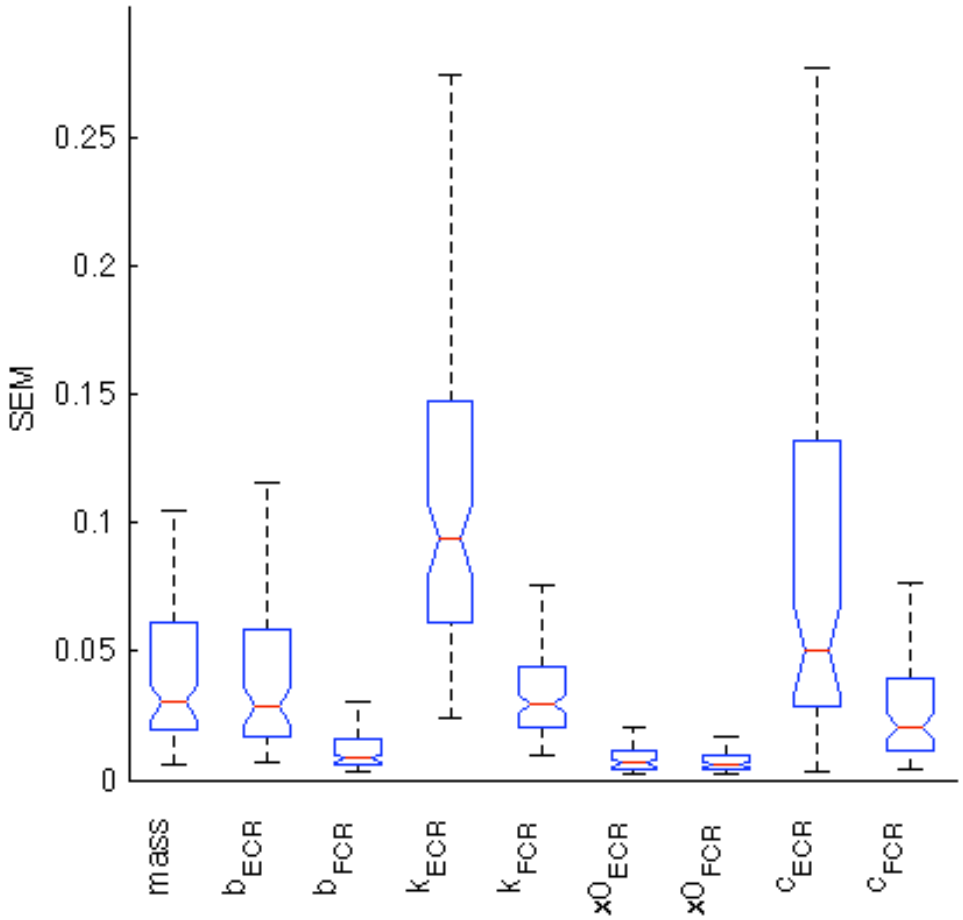

Figure 9: Boxplot of the SEM values of all parameters, except EMG weighting factors. Number of outliers of in total 90 points: mass 6, b_{ECR} 7, b_{FCR} 9, k_{ECR} 8, k_{FCR} 8, $x0_{ECR}$ 11, $x0_{FCR}$ 13, c_{ECR} 13 and c_{FCR} 13.

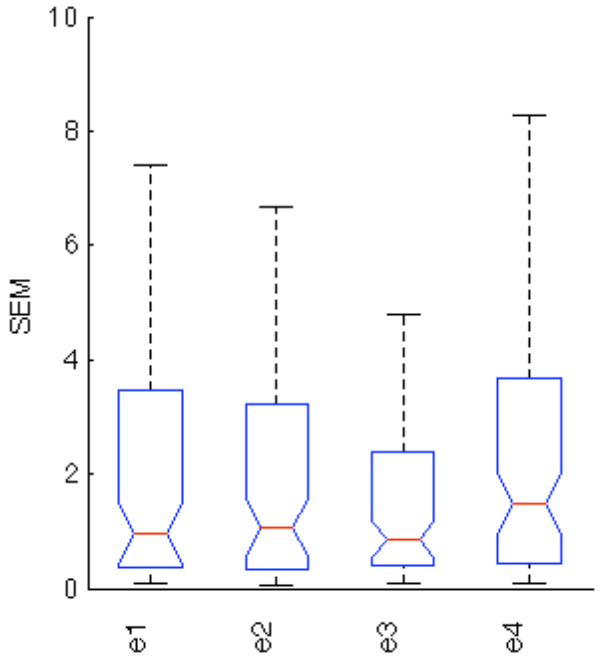

Figure 10: Boxplot of SEM values of the EMG weighting factors. Number of outliers of in total 90 points: E1 9, E2 12, E3 9 and E4 11.

The passive tissue stiffness of healthy subjects was 0.41 ± 0.38 Nm/rad (mean ± 1 s.d.) at 0°. The passive viscosity of healthy subjects was 0.024 ± 0.025

Nm/rad (mean ± 1 s.d) at 0°.

3.3. Method Validity

Forward Simulation of 1 s RaH Rotation

The mean VAF of the forward simulated torque responses to 1 s RaH rotation, in total 92 observations, was 94.1 ± 6.0 (mean ± 1 s.d.), compared to 98.2 ± 2.0 (mean ± 1 s.d.) for the optimized torque response to 0.5 s RaH rotation.

For 15 observations, from 9 patients, the forward simulated torque response was badly predicted (VAF under 70). For 3 patients (5 observations) the fit of the optimized dataset was not very good due to a large difference in wrist torque in hold phase at same angular position between flexion and extension measurements, resulting in low forward simulated fit. For 6 patients (10 observations) the reflex torque in the forward simulated result had extreme responses not present in the measured torque. The results for these 15 observations were not used for further validation of the method.

Forward Simulation of 2nd Visit

The mean VAF of the forward simulated torque response to 1 s RaH rotations of the 2nd visit, in total 68 observations, was 91.3 ± 8.2 (mean ± 1 s.d.), compared to 98.4 ± 2.3 (mean ± 1 s.d.) for the optimized torque response of the 1st visit.

For 10 forward simulated observations (for 5 different patients and 1 control) the VAF values were low (under 70), which were caused by differences in either ROM or torque responses between visits. These 10 observations were not included in the validation since they either represent difference in patient's condition or possibly slightly different arm position between visits that can alter the measured wrist behavior. For patients with modified Ashworth score higher or equal to 2, the repeatability of the wrist torque response between visits can be low (different torque response between visits, indicating changes in the properties of the wrist). Therefore the model cannot capture these abnormal systematic changes. Therefore these patients are not suitable for method validation.

3.4. Difference between Patients and Controls

3.4.1. Torque from Muscle Activation

The torque (r.m.s.) due to offset muscle activation (for both ECR and FCR during extension and flexion rotations of the wrist can be seen in Figure 11. The torque from the ECR offset activation was higher for the patient group, both in extension rotation (U=651, p=0.015) and flexion rotation (U=610, p=0.008). There was no difference in the torque from the FCR offset activation between patients and controls for, neither in extension rotation (U=776, p=0.209) nor flexion rotation (U=805, p=0.312).

The reflexive torque for both ECR and FCR during extension and flexion rotation of the wrist can be seen in Figure 12. There is no difference in the ECR reflex torques between patients and controls, neither in extension rotation (U=860, p=0.581) nor flexion rotation (U=849, p=0.516). The FCR reflexive torque was increased in the patients compared to controls in both extension rotation (U=521, p=0.001) and flexion rotation (U=585, p=0.004). The reflexive response is highest for the FCR during extension rotation, when the muscle is being stretched.

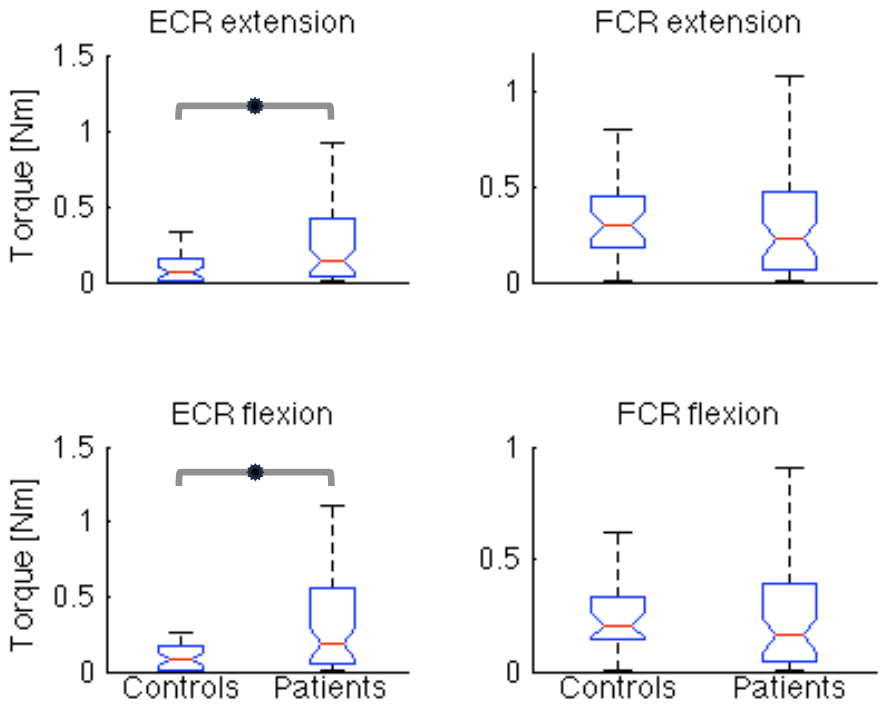

Figure 11: Torque response due to offset muscle activation of patients and controls, for both ECR and FCR during flexion and extension rotations. Number of outliers of in total 33 control subjects: ECR extension 2, ECR flexion 4, FCR extension 0, FCR flexion 0. Number of outliers of in total 57 patients: ECR extension 1, ECR flexion 1, FCR extension 2, FCR flexion 2. The asterisk denotes statistical difference.

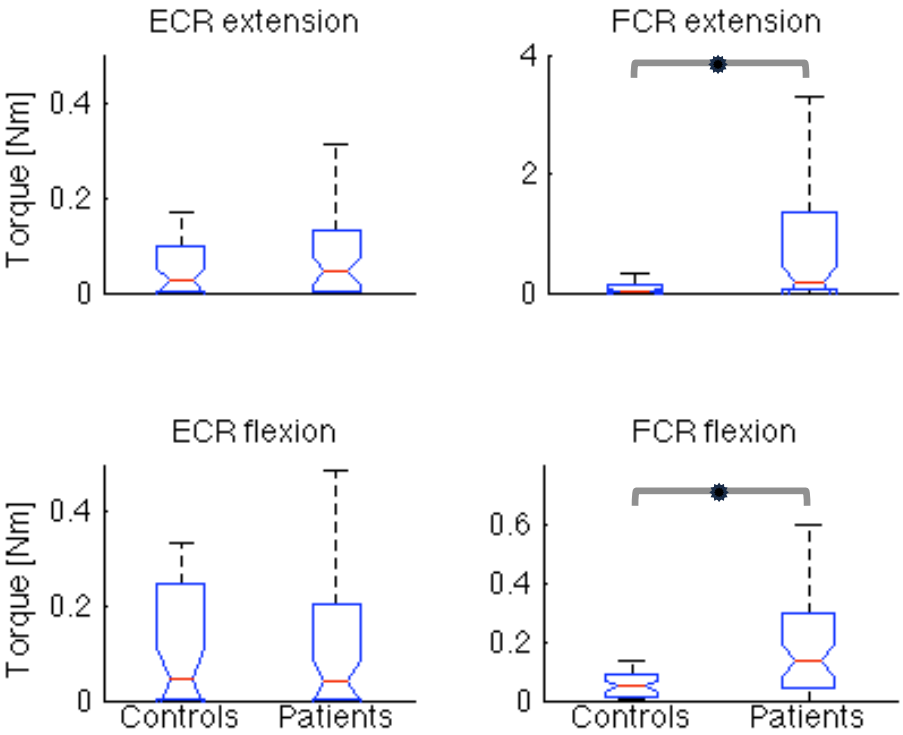

Figure 12: Reflexive torque response of patients and controls, for both ECR and FCR during flexion and extension rotation. Number of outliers of total 33 control subjects: ECR extension 2, ECR flexion 2, FCR extension 3, FCR flexion 6. Number of outliers of total 57 patients: ECR extension 4, ECR flexion 5, FCR extension 0, FCR flexion 4. The asterisk denotes statistical difference.

3.4.2. Torque from Passive Tissues

The one-point viscosity and stiffness of patients and controls are plotted in Figure 13 for the two different angles, $\theta_{comp,flex} = 85°$ and $\theta_{comp,ext} = -55°$, chosen for comparison. In flexed position (ECR properties dominant) the viscosity is not different between patients and controls (U=843.5, p=0.442). In extended position (FCR properties dominant) the viscosity of the patients is higher than of controls (U=689, p=0.046). There is not a difference in stiffness between patients and controls, neither in flexed position (U=908, p=0.892) nor extended position (U=862, p=0.598).

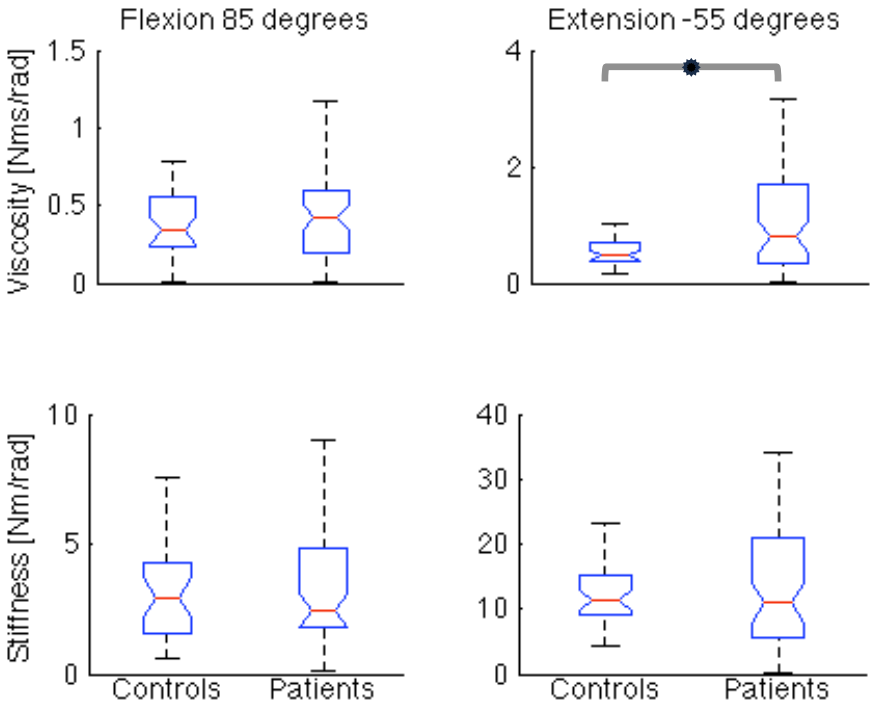

Figure 13: Viscosity and stiffness of the wrist joint in two different positions. The left column shows the viscosity and stiffness in flexion of 85°. The right column shows the viscosity and stiffness in extension of -55°. Number of outliers of in total 33 control subjects: viscosity in flexion 0, stiffness in flexion 2, viscosity in extension 3, stiffness in extension 5. Number of outliers of total 57 patients: viscosity in flexion 6, stiffness in flexion 4, viscosity in extension 5, stiffness in extension 6. The asterisk denotes statistical difference.

The torque contribution from the stiffness of passive tissues for all subjects, was plotted as function of the muscle length over the full ROM (average ROM of control subjects, -55° to 85°), see Figure 14. For comparison the shape of the force-length relationship of active muscle tissue of the ECR and FCR was also plotted in the figure. The median curves for patients and controls (by using the median parameter values) are also plotted. There is a larger variance in the patient curves than for the controls, where the ECR stiffness torque curves for the patients are mainly in the lower range (closer to zero) of the controls. For the FCR the curves of the patients are both in the lower range of the controls and higher than the range of the controls.

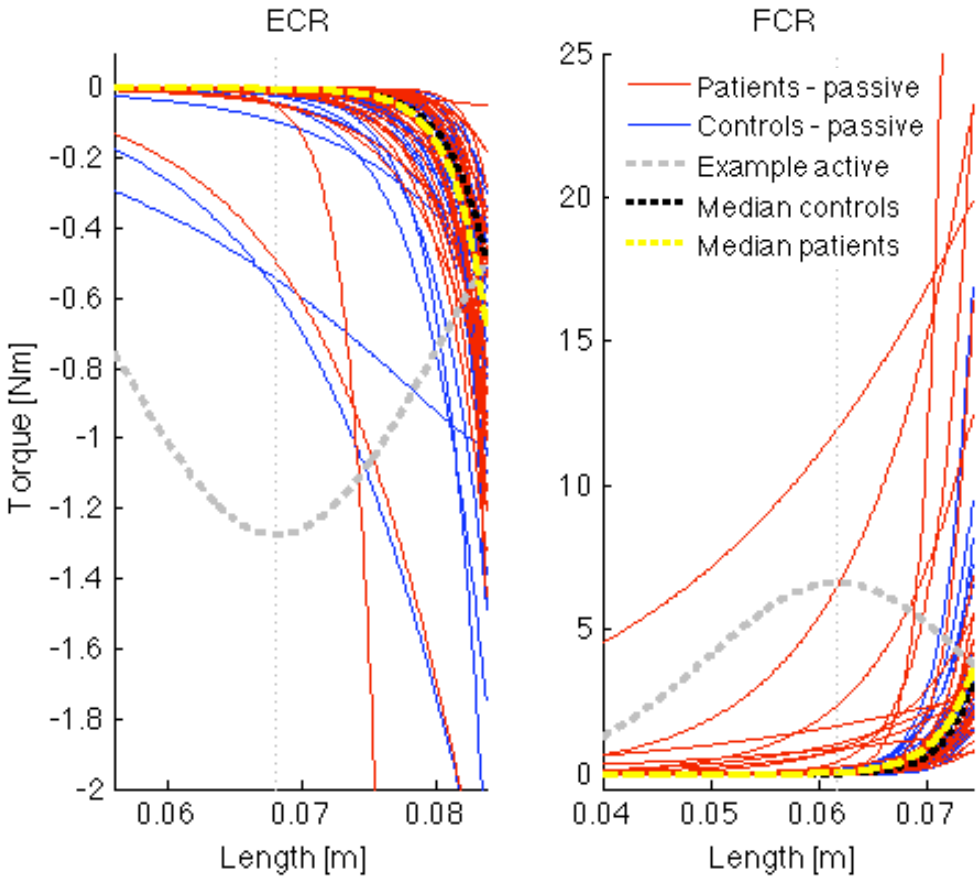

Figure 14: The torque contribution from force-length relationship of passive tissues of all subjects plotted as function of the muscle length, with typical torque from the force-length relationship of active muscle tissue to compare the behavior of the active and passive torques of the force-length relationships of the joint. Left figure shows the torque response from the ECR and the right figure shows the torque response from FCR. For both muscles the optimum length is plotted as a vertical line.

The optimized values of the passive parameters, b, k and x_0, for patients and controls can be seen in Figure 15. There was no difference in the viscosity coefficient, b_{ECR}, between patients and controls (U=786, p=0.241) while b_{FCR} was increased in patients compared to controls (U=672, p=0.025). There was no difference in the stiffness coefficient, k_{ECR}, between patients and controls (U=870, p=0.646), while k_{FCR} was decreased in patients compared to controls (U=586, p=0.004). The muscle force shift parameter of the ECR, $x_{0,ECR}$, was not different between patients and controls (U=870, p=0.646). On the other hand, the muscle force shift parameter of the FCR, $x_{0,FCR}$, was decreased in patients compared to controls (U=586, p=0.004).

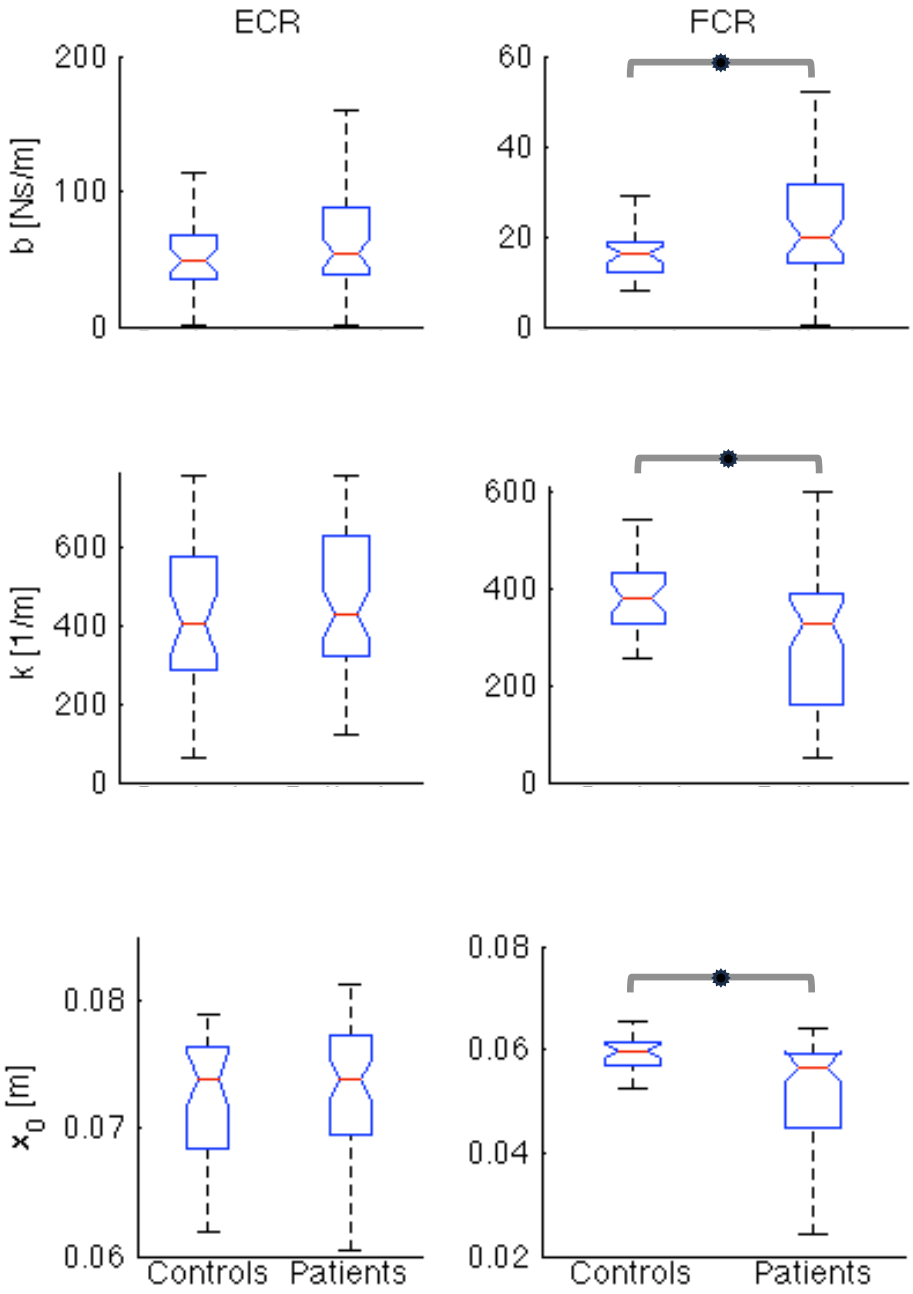

Figure 15: Parameter values of passive tissue properties for both controls and patients. The left column shows the parameter values for the ECR and the right column shows the parameter values for the FCR. First row shows the viscosity parameter, b. Second row shows the stiffness parameter, k. The third row shows the muscle force shift, x_0. Number of outliers of in total 33 control subjects: b ECR 1, b FCR 2, k ECR 0, k FCR 1, x_0 ECR 3, x_0 FCR 0. Number of outliers of total 57 patients: b ECR 10, b FCR 7, k ECR 0, k FCR 0, x_0 ECR 2, x_0 FCR 5. The asterisk denotes statistical difference.

4. Discussion

The main goal of this study was to estimate the offset wrist muscle activation in stroke patients and healthy controls while the wrist joint was at rest. A nonlinear neuromuscular model of the wrist joint was developed. The model separated the components contributing to the wrist torque into neural and non-neural parts. The neural part represents the actual muscle contraction in response to a neural input. The neural input was assumed to be a combination of offset muscle activation, reflexes and voluntary input. In the measurements used for this study

the subjects were instructed to relax, so the voluntary input was assumed to be zero. The non-neural part was separated into the stiffness and viscosity of connective tissues within and surrounding the muscle.

4.1. Offset Muscle Activation at Rest

For both control subjects and stroke patients there was muscle activation at all times, i.e. a nonzero offset in muscle activation even though the subject was instructed to relax. This indicates that the previous studies, where the muscle activation was assumed to be zero when the subjects relaxed the joint of interest, did in fact not take into account an important part of the system, contributing to the total dynamical behavior of the joint.

The shape of the torque curve of the offset muscle activation (see Figure 7 and Figure 8) can be related to the force-length relationship of active muscles. Of course this behavior of contracting muscle is also present in reflexive/voluntary muscle contraction but can be clearly visualized in this case since the offset activation was assumed to be constant. This curve could be used for in vivo estimation of the optimum muscle length, and thus be used to estimate an important property of the muscle. In order to add the optimum muscle fiber length to the parameter optimization a richer data would be needed, such as from active tasks with rotations at different velocities.

4.2. Comparison between Controls and Patients

The patient group was very diverse, with modified Ashworth score from 0-4, leading to large differences between the results of the patients compared to the control group.

The offset muscle activation of stroke patients was similar to controls in the FCR but increased in the ECR. The FCR reflex torque was higher in patients than controls. Also, the FCR reflexive response was a lot higher in extension rotation when the muscle is being stretched, than when tension is released during flexion rotation. The results indicate that hyper reflexive response to a stretch in passive condition was more common in patients than controls, and especially in the FCR and to less extent the ECR. The fact that the reflexive response of the FCR and the ECR offset muscle activation were increased in patients may indicate that the offset activation was a compensation for the hyper reflexive response towards a normal neutral wrist position. Another possible course of action is that originally there might be an offset activation to both the FCR and the ECR. Due to the larger cross-sectional area of the FCR it is stronger than the ECR, which results in higher muscle force. This unbalanced force relation on either side of the wrist could cause change in resting angle, leading to a constant stretch of the ECR and decreased length of the FCR. The decreased length of the FCR results in less rotation needed for proprioceptive feedback from the muscle, increasing the reflex activity.

The cause of the abnormal neural excitations, causing the hyperactive reflexes and increased offset excitation, is not well understood. Recent studies have linked persistent inward current (PICs) in motoneurons to spasticity following spinal cord injury. PICs cause high activation in motoneurons with sustained depolarization (plateau potentials) and neural firing (self-sustained firing) (Bennett et al., 2001; Heckmann et al., 2005; Hultborn et al., 2004). In healthy subjects neuromodulatory signals from the brainstem (e.g. serotonin and norepinephrine) control the activation of the PICs, regulating normal movement

patterns and preventing too much neural activation to the muscles. The signals from the brainstem can be disrupted following spinal cord injury causing decreased excitation threshold, uncontrolled firing, muscle clonus and hyperactive reflexes (Bennett et al., 2001; Heckmann et al., 2005). Possibly these abnormalities can be linked to the hyperactive reflexes following stroke (Hultborn et al., 2004).

The one-point comparison of passive stiffness and viscosity between patients and controls at $\theta_{comp,flex}$ and $\theta_{comp,ext}$ show that there was larger difference between the two groups in extended position. The passive viscosity and stiffness of the ECR (dominant in flexed position) was similar between patients and controls with a slightly increased range of results for the patients. In the extended wrist position, where the main passive response comes from the FCR, the difference between patients and controls is larger. Only the viscosity was though significantly larger in the patients than controls. For both viscosity and stiffness the patients had broader range of results, both towards higher and lower viscosity and stiffness. This indicated that there were more structural tissue changes within the FCR than the ECR following stroke.

The drawback of choosing one point of the stiffness and viscosity curve for comparison between subjects is that this one point might give misleading information about the overall behaviour of the viscoelasticity. Due to the nonlinear relationship and the two (or three in case of viscosity) parameters that define the different properties of the stiffness torque curve (steepness and shift of the curve) there is a possibility of an intersection of the curves of different subjects. In these cases the quantification of the patients' stiffness torque depends on which side of the intersection point the angle of comparison is. Therefore using this one-point analysis for diagnosis might give misleading information about the actual underlying mechanism, that is, no information are derived if the changes in stiffness are caused by changes in tissue stiffness (determined by k) or length of tissues (determined by x_0). Due to this fact the actual parameter values were also be used to compare patients and controls, in order to gain information about what changes occur in the tissues that cause the altered viscoelastic behaviour.

Indeed, by looking into the optimized parameter values of the passive tissue properties, b, k and x_0, it came clear that all parameters of the FCR changed for the stroke patients compared to the controls, but none of the parameters of the ECR. These were not the same results as derived with the one-point analysis, where the stiffness torque was not significantly different between patients and controls, neither for the FCR nor the ECR. This supports the statement in the previous paragraph; that by looking into the parameter values instead of the stiffness torque at one point, information about the overall behavior of the passive tissues can be derived. The increase in the viscosity coefficient, b_{FCR}, indicated a possible change in tissue composition within the muscle leading to altered viscous behavior, since some studies have shown increased amount of intracellular fat deposition (Hafer-Macko et al., 2008) and extracellular matrix in muscle bundles of spastic muscles (Lieber et al., 2003). By looking at Figure 14 for the FCR, it can be seen that for many patients the stiffness torque curve is shifted upwards (decreased x_0) and with low steepness (decreased k). This change in the shape of the stiffness torque curve was also represented in the change of optimized parameter values, where k and x_0 were decreased for the stroke patients compared to the controls. This change in passive parameter values for the FCR

might indicate an increase in passive connective tissues in the in stroke patients. Also, the decrease in x_0 can indicate shortening of the muscle and connective tissues, causing the start of the exponential rise of the stiffness torque curve at smaller length change. The possible shortening of the FCR might also partly explain the increased reflex activity of the muscle, since for shorter muscle less length change is needed to activate the proprioceptors. Together with the possibly decreased excitation threshold of the PICs these length changes could lead to the increased reflex activity of the FCR.

4.3. Verification and Validation of the Method

The model was internally verified with VAF and SEM values. The method was validated with two different forward simulations; different input signals applied in same visit and same input signal applied in two different visits. The high VAF values of the forward simulated torque responses indicate that the model is good in predicting the total torque response and separate it into its underlying factors, both for healthy subjects and stroke patients, from less to more severely affected.

As stated before, some observations were discarded from the forward simulation of different RaH rotation due to bad fit caused by extreme reflex torque not present in the measured torque. This overestimation is most likely due to the fact that the relation between force and EMG response is nonlinear, but since the neural parameters are fixed in the forward simulation a linear relation is applied. Therefore a change in EMG signal between the two different measurements can lead to overestimation of the resulting force. If the nonlinear relationship between muscle force and EMG for each subject were estimated and included in the model it might be more suitable to predict the muscle force at different conditions.

In the forward simulation of the 2nd visit some observations were discarded due to low repeatability between visits, meaning that despite from measuring the same subject at the same condition the measured torque or the ROM had changed to a large extent. In other observations that had poor model fit despite for high repeatability between visits, the reason for the poor fit was the exponential curve of the passive tissue stiffness. In cases where the optimized stiffness coefficient k is high, a slight change in ROM can have large effects on the torque contribution from the force-length relationship of passive tissues. This can lead to extremely high or low stiffness torques and therefore bad model fits. This was the cause of low VAF for many other observations than the ones that were removed from the analysis, only with less extreme effects. That means that the dynamical behavior of the wrist was well represented but with a slight shift in total torque due to the stiffness contribution.

By looking at the SEM values in Figure 10, it is clear that for most parameters the SEM values are higher for the ECR than the FCR. A possible cause is the restricted amount of information about the ECR that are present in the data, due to the commonly reduced ROM in the extension direction. More likely reason for lack of information about the ECR is its low stiffness and viscosity compared to the FCR, which indicates that the ECR is slacker than the FCR. That means that the rotation over the full ROM might not fully stretch the ECR and the maximum flexion angle depends on other structures of the joint (not included in the model), such as bony structures inside the joint preventing further wrist rotation. If the muscle is not stretched close to the end range, the exponential relationship might not be clear and only a small part of the mechanical properties of the muscle is

observed. In order to accurately estimate a part of the system, the relative part needs to be well represented in the data. A different measurement (e.g. during active task) might increase information about the viscoelastic properties of the ECR in the data, resulting in more accurate parameter estimation.

4.4. Comparison to Literature

For model validation, stiffness and viscosity of healthy subjects was found in literature and compared to the modelled stiffness and viscosity, derived with one-point analysis. In literature the wrist stiffness at neutral position (0°) for healthy subjects was found to be in the range of 0.32-3 Nm/rad (De Serres & Milner, 1991; Gielen & Houk, 1984; Rijnveld & Krebs, 2007). Since no information about wrist stiffness in stroke patients was found only the results for healthy subjects were used for validation. The modeled passive tissue stiffness of healthy patients was 0.41 ± 0.38 Nm/rad (mean ± 1 s.d.), which is close to the lower range of the stiffness found in literature.

The passive tissue viscosity of the wrist joint in flexion-extension movement in healthy subjects has been found to be 0.03 Nms/rad (Charles & Hogan, 2011), and for the same reason as before only the results from healthy subjects were used for validation. The modeled passive viscosity of healthy patients was 0.024 ± 0.025 Nm/rad (mean ± 1 s.d.), which is slightly lower than found in literature.

Care should be taken that in previous studies, torque from background muscle activation was not separated from the total passive torque. This means that the torque contribution from the constant active part has in previous studies might have been added to the passive part causing slightly higher estimated stiffness and viscosity than found in this study. All the studies found that linked the EMG to the joint torque in order separate the contributing parts, and compared stroke patients and healthy subjects, analyzed the ankle joint. Since the behavior of the wrist joint and the ankle joint are different it is not possible to compare the results directly. The results of de Vlugt et al. (2010) showed increased ankle torque due to tissue stiffness, which is not in accordance with the results of this study. On the other hand decrease in tissue stiffness of the wrist has been reported before with other research methods (Meskers et al., 2009), which supports the results of this study.

4.5. Clinical Implications

The method used in this study, with instrumented test and full separation of the neuromuscular components contributing to the joint torque, improves the possible diagnosis of the movement disorder following stroke. By separating the offset muscle activation, in addition to the reflexive activity and passive stiffness and viscosity, the clinician would have a better guide to choose the optimal treatment for each patient.

By looking into the parameters of the passive tissue viscoelasticity, instead of using one-point analysis, more information can be derived about the origin of the change in the behavior of passive tissues. For example, if a patient has highly increased stiffness parameter k, a thinning of the tendon might be an applicable treatment, but if the force shift length x_0 has decreased, a lengthening or release of muscle might be optimum treatment.

In addition, the new method can be used to study the effects of treatment methods on the parts contributing to the wrist torque, by analyzing the patients' condition before and after the application of a therapy. This might give new

information about the different treatment methods, if they have positive, negative or no effects on each part of the joint torque. Also, this method might be used for studying the suitable treatment doses of medicine, e.g. Botolinum Toxin-A injections.

4.6. Limitations

By using two observations for each optimization, that is, both flexion and extension rotations, which enriches the information used to analyze the system. On the other hand, since the joint behaves in highly nonlinear manner, the torque in the same position might not be equal in both observations, e.g. due to tissue hysteresis. This enforces the model to compensate the fit in between the torque responses from both observations, which leads to lower VAF than if only one observation was used for every optimization. Concluded, using two observations for every optimization adds information to the model but also restricts it in cases where the joint response changes with time and previously performed movements. The model fit might improve if the hysteric behavior of connective tissues was included in the model.

In this study the minimum average EMG over the whole observation time was taken as the offset muscle activation. This was estimation and a small reflexive or voluntary excitation might be added to the actual offset at the minimum EMG signal. Although a full separation between the offset and varying part was not guaranteed, it takes into account that the system is highly non-linear and the EMG signal is not necessarily the same in same position, but depends on previous activities. Therefore it was not assumed that the EMG signal before the onset of rotation was solely offset excitation and the current solution was the best one available at this state.

In the forward simulation of the 2nd visit a part of the parameters were optimized again, giving the model freedom to solve any misfits in parameters with the new optimized values, so this was not a full forward simulation. This was a drawback, but on the other hand the only way to sufficiently validate the method between visits due to the difference in EMG electrode placement.

Additionally, for the forward simulation of the 2nd visit the VAF values were on average lower than for the forward simulation of different RaH rotations. A possible reason could be a slight difference in configuration of the patients in the measurement device between visits. It's suggested that exact placement will be noted in first visit and applied again for next visits in order to ensure consistency in measurement setup. These variables are the height of the elbow rest, position of elbow paddle and position of rotating handle. This would prevent changes in the measured torque response between visits, which do not origin in the dynamical behavior of the wrist.

In the forward simulation of the different RaH rotations it came clear that the model does not capture the full relationship between muscle EMG and wrist torque, since in some cases the force from the active part was overestimated. The weighting factors (e_1, e_2, e_3, e_4), fixed from optimization to forward simulation, assume linear relationship between muscle EMG and muscle force, which is not the case. In order to improve the model so that it can be used to predict the wrist dynamics at different conditions the nonlinear relationship between muscle EMG and muscle force would need to be captured.

4.7. Future Research

In this study, data from passive measurements was used, that is, the subject's task was to remain relaxed. The joint characteristics in active conditions are not fully understood (Burne et al., 2005; Mirbagheri et al., 2001) and play bigger role in the movement disorder (Burne et al., 2005). Applying the model to data from active measurement might give more valuable information about the joint torque. Choosing treatment depending on active assessment might improve the patient's functional ability to higher extent than by using passive assessments. Therefore, for further analysis a different measurement is recommended. Measurement during force task, while applying position perturbations at different velocities might enrich the information of the data, increasing the potential of the model, e.g. to estimate the optimum muscle length and the activation cutoff frequency.

In this study the minimum EMG signal (after removing the measurement noise) was assumed to represent the offset muscle activation. It is not known if a passive task is necessary to find the minimum muscle activation. Possibly only an active task is needed since the minimum activation of a muscle (antagonist) can be seen during voluntary activation of the agonist, due to reciprocal inhibition of the antagonist, suppressing its reflex activity. In spastic patients this suppression can be lost leading to large reflex activity in the antagonist during voluntary activation of the agonist (Boorman et al., 1996). Therefore it needs to be tested if a combination of passive and active task is needed to identify the offset activation, or if an active task provides sufficient information, before deciding next steps with this new method.

5. Conclusion

This study introduced a new method for quantification of the neuromuscular properties of the wrist joint, in flexion and extension rotations. In addition to the reflexive muscle activation and the stiffness and viscosity of passive tissues, estimated in previous studies, this method enabled separation of the offset muscle activation. The model and the method have been validated and succeeded in quantifying the parts of the neuromuscular system contributing to the wrist torque.

Offset muscle activation was present in both patients and controls at rest. The results of this study revealed increased offset muscle activation of the ECR, altered tissue viscoelasticity and reflex activity of the FCR in stroke patients. This can indicate a counterbalance of increased constant muscle activation of the ECR to compensate for the change in neutral position, caused by muscle shortening (causing increased reflex activity) and altered tissue viscoelasticity of the FCR (or vice versa). To conclude, a new antagonistic force balance had developed around the wrist joint following stroke, causing changed neutral position, with a structural origin on one side and an active (neural origin) on the opposite side.

The results indicate the importance of estimating the offset muscle activation contributing to the wrist torque. This new method provides additional information about the origin of the movement disorder following stroke, facilitating the choice of a treatment method when choosing for casting, drug therapy or surgical intervention.

Appendix 1: Neuromuscular Model

The wrist joint torque response is described with:

$$T_{mod}(t) = I\ddot{\theta}(t) + T_{FCR}(t) - T_{ECR}(t) \qquad A1$$

where t is the independent time variable [s]. T_{mod} is the modeled total torque from the wrist [Nm], T_{FCR} and T_{ECR} are the torque contributions from the flexor and extensor carpi radialis [Nm], respectively. I is the inertia of the hand and the handle [kg.m^2] and $\ddot{\theta}(t)$ is the angular acceleration of the wrist [rad/s^2].

The torque response from each muscle is modeled by taking into account the passive and active muscle properties.

$$T_{FCR}(t) = \left(F_{visc,FCR}(x,\dot{x}) + F_{stiff,FCR}(x) + F_{active,FCR}(t)\right) r_{FCR}(\theta) \qquad A2$$

$$T_{ECR}(t) = \left(F_{visc,ECR}(x,\dot{x}) + F_{stiff,ECR}(x) + F_{active,ECR}(t)\right) r_{ECR}(\theta) \qquad A3$$

where x is the change of muscle length [m] and $\dot{x}$ is the rate of the change of muscle length [m/s]. F_{visc} is the muscle force that is related with velocity to the viscosity of passive tissues [Ns/m], F_{stiff} is the muscle force that is related with length to the stiffness of the passive tissues [N/m] and F_{active} is the muscle force from the active muscle tissue. The $r_{FCR}(\theta)$ and $r_{ECR}(\theta)$ are the moment arms [m] of the FCR and ECR respectively, and they are dependent on the angular position of the joint, found with (Ramsay et al., 2009):

$$r_{FCR}(\theta) = (13.2040 + 1.5995\theta)10^{-3} \ [m] \qquad A4$$

$$r_{ECR\ brevis}(\theta) = (13.4337 - 2.1411\theta)10^{-3} \ [m] \qquad A5$$

$$r_{ECR\ longus}(\theta) = (11.7166 - 2.2850\theta)10^{-3} \ [m] \qquad A6$$

$$r_{ECR}(\theta) = \frac{r_{ECR\ brevis}(\theta) + r_{ECR\ longus}(\theta)}{2} \qquad A7$$

The ECR is in fact two separate muscles, extensor carpi radialis longus and brevis, but since only a combined EMG signal can be measured the extensor moment arm is assumed to be the average of the two separate moment arms.

The lengths of the muscles change with position, derived with the following equations:

$$x_{FCR} = l_{FCR} - r_{FCR}(\theta) \cdot \theta \qquad A8$$

$$x_{ECR} = l_{ECR} + r_{ECR}(\theta) \cdot \theta \qquad A9$$

where x_{FCR} and x_{ECR} are the lengths of the muscle at each position θ and l_{FCR} and l_{ECR} are the optimum muscle lengths and $r_{FCR}(\theta) \cdot \theta$ and $r_{ECR}(\theta) \cdot \theta$ are the arc lengths of the tendon that stretches around the joint bone when the joint rotates about angle θ (Lieber et al., 1997). Positive angles represent flexion, thus the FCR shortens during flexion and the ECR lengthens, and vice versa for the extension. A schematic representation of this length change can be seen in Figure

16. For simplification it is assumed that the same relation applies for the full range of motion.

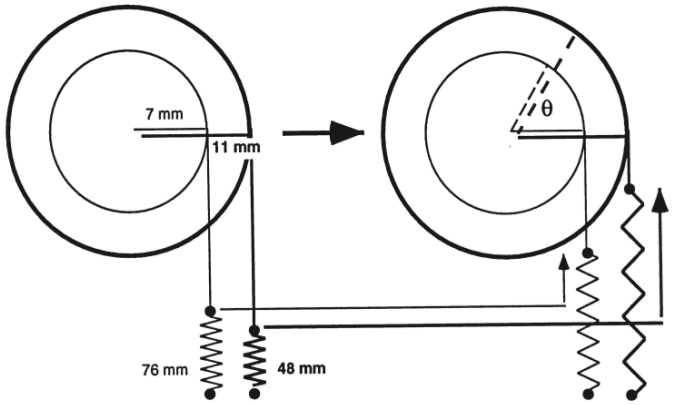

Figure 16: The interrelation between muscle moment arm and the change in fiber length with rotation, for extensor carpi radialis brevis and extensor carpi radialis longus. The schematic diagram of the wrist joint shows the change from neutral position to extended position. The joint is represented as two concentric circles where the moment arms are the radii. From Lieber, 1997.

The inertia of the hand and the handle is modeled as a point mass m [kg] in distance l_a, 0.04 [m] (Lemay & Crago, 1996), from the axis of rotation:

$$I = ml_a^2 \qquad A10$$

The viscosity and stiffness components from the flexor carpi radialis are modeled with (de Vlugt et al., 2010):

$$F_{visc,FCR}(t) = e^{k_{FCR}\left(x_{FCR}(t)-x_{0,FCR}\right)}\dot{x}_{FCR}(t)b_{FCR} \qquad A11$$

$$F_{stiff,FCR}(t) = e^{k_{FCR}\left(x_{FCR}(t)-x_{0,FCR}\right)} \qquad A12$$

and similar for the extensor carpi radialis. Both the viscous and stiffness forces depend on the wrist position, with an exponential relation. The amount of viscous force is defined by the viscosity coefficient b [Ns/m]. The shape of the exponential stiffness curve is defined by k [1/m]. In order to enable a shift in the viscous and stiffness forces a shift parameter, x_0 [m], is included. It determines at what muscle length the force starts increasing exponentially.

The stiffness and viscosity of the wrist, K_{joint} [Nm/rad] and B_{joint} [Nms/rad], were calculated at a certain angle, θ_{comp}, for all subjects and compared to literature. The stiffness of the FCR was found with (de Vlugt et al., 2010):

$$K_{joint,FCR} = \frac{dT_{stiff}}{d\theta} = \frac{dF_{stiff,FCR}r_{FCR}(\theta_{comp})}{dx \Big/ r_{FCR}(\theta_{comp})}$$
$$= k_{FCR}e^{k_{FCR}\left(x_{FCR,comp}(t)-x_{0,FCR}\right)}r_{FCR}^2(\theta_{comp}) \qquad A13$$

where k_{FCR} and $x_{0,FCR}$ were derived with the model and $x_{FCR,comp}$ is the muscle length at θ_{comp}. The stiffness of the ECR was derived in the same way.

The total joint stiffness was derived by adding the stiffness from both muscles, respectively:

$$K_{joint,} = K_{joint,FCR} + K_{joint,ECR} \qquad A14$$

The viscosity of the FCR was found with (de Vlugt et al., 2010):

$$B_{joint,FCR} = \frac{dT_{stiff}}{d\dot{\theta}} = \frac{dF_{stiff,FCR} r_{FCR}(\theta_{comp})}{d\dot{x} \Big/ r_{FCR}(\theta_{comp})}$$
$$= b_{FCR} e^{k_{FCR}(x_{FCR,comp}(t) - x_{0,FCR})} r_{FCR}^2(\theta_{comp}) \qquad A15$$

where b_{FCR}, k_{FCR} and $x_{0,FCR}$ were derived with the model and $x_{FCR,comp}$ is the muscle length at θ_{comp}. The viscosity of the ECR was derived in the same way. The total joint viscosity was derived by adding the viscosities from both muscles, respectively:

$$B_{joint,} = B_{joint,FCR} + B_{joint,ECR} \qquad A16$$

The same equations (A13-A16) were used to calculate the stiffness and viscosity at the two different angles, $\theta_{comp,flex} = 85$ and $\theta_{comp,ext} = -55°$, to compare the patients and controls.

The neural muscle activity of both the FCR and the ECR was estimated from the IEMG signals from the measurements. In this study the IEMG signal was assumed to consist of three parts; the offset excitation, the varying excitation (reflexive/voluntary) and measurement noise part. To remove the noise from the measured IEMG parameters were added to the model ($c_{noise,FCR}$ and $c_{noise,ECR}$), which allowed the model to estimate the part of the IEMG that did not contribute to the wrist torque. The neural excitation that does correspond to the wrist torque (offset and varying excitation) was found by subtracting the noise from the measured IEMG:

$$u_{FCR} = e_1 IEMG_{FCR,dist}(t) + e_3 IEMG_{FCR,prox}(t) - c_{noise,FCR} \qquad A17$$

$$u_{ECR} = e_2 IEMG_{ECR,dist}(t) + e_4 IEMG_{ECR,prox}(t) - c_{noise,ECR} \qquad A18$$

where u_{FCR} and u_{ECR} are the modeled neural muscle excitations of the flexor carpi radialis and the extensor carpi radialis respectively, $e_1 - e_4$ are optimized weighting factors [N/V] to estimate the offset and reflexive excitations and the IEMG are the measured muscle EMG for the electrodes placed distally and proximally on each muscle. The $c_{noise,FCR}$ and $c_{noise,ECR}$ are the optimized constants to remove the measurement noise from the neural muscle excitations signals of the FCR and the ECR respectively.

The neural excitations of both muscles were filtered with a linear second order filter in order to describe the activation process of a contracted muscle (de Vlugt et al., 2010):

$$\alpha_{FCR}(s) = \frac{\omega_0^2}{s^2 + 2\beta\omega_0 s + \omega_0^2} u_{FCR}(s) \qquad A19$$

and the same filter was used for the ECR. α_{FCR} represents the active state of the flexor carpi radialis, $\omega_0 = 2\pi f_0$ is the cutoff frequency of the filter where f_0 was set as 2.17 Hz (Schouten et al., 2008), s is the Laplace operator and $u_{FCR}(s)$ is the modeled neural muscle activity of the FCR (see subchapter 2.2). The relative damping factor, β, was set to 1, so the system is critically damped (de Vlugt et al., 2010).

Hill-type muscle model was used to estimate the muscle force from the neural muscle activity (combination from both offset and varying activation), muscle length and velocity (de Vlugt et al., 2010):

$$F_{active,FCR} = f_v(v_{FCR}) f(l_{FCR}) \alpha_{FCR} \qquad A20$$

The same was used for the extensor carpi radialis. The optimum muscle lengths were $l_{FCR} = 6.3cm$ and $l_{ECR} = 7.0cm$ (average of optimum muscle length of ECR brevis and ECR longus) (Holzbaur et al., 2005). The optimum muscle length was used to derive the force-length relationship, the maximum shortening velocity was 8 times the optimum muscle length, the maximum eccentric force was 1.5 times the isometric force and the isometric force was normalized to 1 because the force had been scaled by the weighting factors $e_1 - e_4$.

The total active muscle force contains both the contribution from offset muscle activation and reflexive muscle activation. In order to separate these the offset excitation, $u_{FCR,off}$, was filtered with the activation filter, see equation A19. Then the offset muscle activation, $\alpha_{offset,FCR}$, was fed to the Hill-type muscle model, resulting in the offset muscle force:

$$F_{offset,FCR} = f_v(v_{FCR}) f(l_{FCR}) \alpha_{offset,FCR} \qquad A21$$

The force from the reflexive muscle activation was found with:

$$F_{reflex,FCR}(t) = F_{active,FCR}(t) - F_{offset,FCR}(t) \qquad A22$$

Similar was done to derive the muscle force from the offset activation and reflexive activation of the ECR. To compare the offset activity and the reflex activity of the subjects the root mean square (r.m.s.) of the modelled offset response and the modelled reflex response was calculated over the observation time. The torque response (r.m.s.) from the neural offset of the FCR was found with:

$$T_{offset,FCR} = \sqrt{\frac{1}{N} \int \left(F_{offset,FCR}(n) r_{FCR}\right)^2} \qquad A23$$

where n represents the time sample of the observation time from 1 to N. The size of N depends on the sample frequency, 2048 Hz, and observation time, which is 1 s from the two hold phases plus the duration of the ramp. The offset torque response from the ECR was found similarly. The torque response from the neural reflexes of both muscles was derived with the same equation.

Reference

Ashworth, B. (1964). Preliminary Trial of Carisoprodol in Multiple Sclerosis. *Practitioner, 192*(115), 540-&.

Belda-Lois, J. M., Mena-del Horno, S., Bermejo-Bosch, I., Moreno, J. C., Pons, J. L., Farina, D., . . . Rea, M. (2011). Rehabilitation of gait after stroke: a review towards a top-down approach. *Journal of NeuroEngineering and Rehabilitation, 8*.

Bennett, D. J., Li, Y., Harvey, P. J., & Gorassini, M. (2001). Evidence for plateau potentials in tail motoneurons of awake chronic spinal rats with spasticity. [Research Support, Non-U.S. Gov't]. *Journal of Neurophysiology, 86*(4), 1972-1982.

Boorman, G. I., Lee, R. G., Becker, W. J., & Windhorst, U. R. (1996). Impaired "natural reciprocal inhibition" in patients with spasticity due to incomplete spinal cord injury. [Research Support, Non-U.S. Gov't]. *Electroencephalogr Clin Neurophysiol, 101*(2), 84-92.

Burne, J. A., Carleton, V. L., & O'Dwyer, N. J. (2005). The spasticity paradox: movement disorder or disorder of resting limbs? *Journal of Neurology Neurosurgery and Psychiatry, 76*(1), 47-54.

Charles, S. K., & Hogan, N. (2011). Dynamics of wrist rotations. *Journal of Biomechanics, 44*(4), 614-621.

De Serres, S. J., & Milner, T. E. (1991). Wrist muscle activation patterns and stiffness associated with stable and unstable mechanical loads. [Research Support, Non-U.S. Gov't]. *Exp Brain Res, 86*(2), 451-458.

de Vlugt, E., de Groot, J., Schenkeveld, K., Arendzen, J. H., van der Helm, F., & Meskers, C. (2010). The relation between neuromechanical parameters and Ashworth score in stroke patients. *Journal of NeuroEngineering and Rehabilitation, 7*(1), 35.

Di Carlo, A. (2009). Human and economic burden of stroke. *Age and Ageing, 38*(1), 4-5.

Dietz, V., & Sinkjaer, T. (2007). Spastic movement disorder: impaired reflex function and altered muscle mechanics. *The Lancet Neurology, 6*(8), 725-733.

Gielen, C. C., & Houk, J. C. (1984). Nonlinear viscosity of human wrist. [Research Support, Non-U.S. Gov't]. *Journal of Neurophysiology, 52*(3), 553-569.

Hafer-Macko, C. E., Ryan, A. S., Ivey, F. M., & Macko, R. F. (2008). Skeletal muscle changes after hemiparetic stroke and potential beneficial effects of exercise intervention strategies. [Research Support, N I H , Extramural, Research Support, U S Gov't, Non-P H S, Review]. *J Rehabil Res Dev, 45*(2), 261-272.

Heckmann, C. J., Gorassini, M. A., & Bennett, D. J. (2005). Persistent inward currents in motoneuron dendrites: implications for motor output. [Review]. *Muscle Nerve, 31*(2), 135-156.

Hof, A. L., & Vandenberg, J. (1981). Emg to Force Processing .1. An Electrical Analog of the Hill Muscle Model. *Journal of Biomechanics, 14*(11), 747-&.

Holzbaur, K. R., Murray, W. M., & Delp, S. L. (2005). A model of the upper extremity for simulating musculoskeletal surgery and analyzing neuromuscular control. *Annals of Biomedical Engineering, 33*(6), 829-840.

Hultborn, H., Brownstone, R. B., Toth, T. I., & Gossard, J. P. (2004). Key mechanisms for setting the input-output gain across the motoneuron pool. *Brain Mechanisms for the Integration of Posture and Movement, 143*, 77-95.

Klomp, A., Van der Krogt, J., Meskers, C. G., de Groot, J. H., de Vlugt, E., van der Helm, F. C., & Arendzen, H. J. (2012). Design of a Concise and Comprehensive Protocol for Post Stroke Neuromechanical Assessment. *J Bioengineer & Biomedical Sci S1:008*

Kwah, L. K., Herbert, R. D., Harvey, L. A., Diong, J., Clarke, J. L., Martin, J. H., . . . Gandevia, S. C. (2012). Passive Mechanical Properties of Gastrocnemius Muscles of People With Ankle Contracture After Stroke. *Archives of Physical Medicine and Rehabilitation, 93*(7), 1185-1190.

Kwakkel, G., Meskers, C. G., van Wegen, E. E., Lankhorst, G. J., Geurts, A. C., van Kuijk, A. A., . . . Arendzen, J. H. (2008). Impact of early applied upper limb stimulation: the EXPLICIT-stroke programme design. *BMC Neurol, 8*, 49.

Lannin, N. A., Cusick, A., McCluskey, A., & Herbert, R. D. (2007). Effects of splinting on wrist contracture after stroke - A randomized controlled trial. *Stroke, 38*(1), 111-116.

Latash, M. L., & Anson, J. G. (1996). What are "normal movements" in atypical populations? *Behavioral and Brain Sciences, 19*(1), 55-+.

Lemay, M. A., & Crago, P. E. (1996). A dynamic model for simulating movements of the elbow, forearm, an wrist. *Journal of Biomechanics, 29*(10), 1319-1330.

Lieber, R. L., Ljung, B. O., & Friden, J. (1997). Intraoperative sarcomere length measurements reveal differential design of human wrist extensor muscles. *J Exp Biol, 200*(Pt 1), 19-25.

Lieber, R. L., Runesson, E., Einarsson, F., & Friden, J. (2003). Inferior mechanical properties of spastic muscle bundles due to hypertrophic but compromised extracellular matrix material. *Muscle & Nerve, 28*(4), 464-471.

Lieber, R. L., Steinman, S., Barash, I. A., & Chambers, H. (2004). Structural and functional changes in spastic skeletal muscle. *Muscle & Nerve, 29*(5), 615-627.

Lloyd, D. G., & Besier, T. F. (2003). An EMG-driven musculoskeletal model to estimate muscle forces and knee joint moments in vivo. *Journal of Biomechanics, 36*(6), 765-776.

Logan, L. R. (2011). Rehabilitation Techniques to Maximize Spasticity Management. *Topics in Stroke Rehabilitation, 18*(3), 203-211.

Meskers, C. G., Schouten, A. C., de Groot, J. H., de Vlugt, E., van Hilten, B. J., van der Helm, F. C., & Arendzen, H. J. (2009). Muscle weakness and lack of reflex gain adaptation predominate during post-stroke posture control of the wrist. *J Neuroeng Rehabil, 6*, 29.

Mirbagheri, M. M., Barbeau, H., Ladouceur, M., & Kearney, R. E. (2001). Intrinsic and reflex stiffness in normal and spastic, spinal cord injured subjects. *Exp Brain Res, 141*(4), 446-459.

Mirbagheri, M. M., Rymer, W. Z., Tsao, C., & Settle, K. (2005). Evolution of reflexive and muscular mechanical properties in stroke-induced spasticity. *Conf Proc IEEE Eng Med Biol Soc, 4*, 4393-4395.

Ramsay, J. W., Hunter, B. V., & Gonzalez, R. V. (2009). Muscle moment arm and normalized moment contributions as reference data for

musculoskeletal elbow and wrist joint models. *Journal of Biomechanics, 42*(4), 463-473.

Renzenbrink, G. J., Buurke, J. H., Nene, A. V., Geurts, A. C., Kwakkel, G., & Rietman, J. S. (2012). Improving walking capacity by surgical correction of equinovarus foot deformity in adult patients with stroke or traumatic brain injury: a systematic review. *Journal of Rehabilitation Medicine, 44*(8), 614-623.

Rijnveld, N., & Krebs, H. I. (2007). Passive wrist joint impedance in flexion-extension and abduction-adduction. *2007 Ieee 10th International Conference on Rehabilitation Robotics, Vols 1 and 2*, 43-47.

Schouten, A. C., De Vlugt, E., Van Hilten, J. J. B., & Van der Helm, F. C. T. (2008). Quantifying proprioceptive reflexes during position control of the human arm. *Ieee Transactions on Biomedical Engineering, 55*(1), 311-321.

Sinkjaer, T., & Magnussen, I. (1994). Passive, intrinsic and reflex-mediated stiffness in the ankle extensors of hemiparetic patients. [Research Support, Non-U.S. Gov't]. *Brain, 117 (Pt 2)*, 355-363.

Smith, L. R., Lee, K. S., Ward, S. R., Chambers, H. G., & Lieber, R. L. (2011). Hamstring contractures in children with spastic cerebral palsy result from a stiffer extracellular matrix and increased in vivo sarcomere length. *Journal of Physiology-London, 589*(10), 2625-2639.

Sommerfeld, D. K., Gripenstedt, U., & Welmer, A. K. (2012). Spasticity After Stroke An Overview of Prevalence, Test Instruments, and Treatments. *American Journal of Physical Medicine & Rehabilitation, 91*(9), 814-820.

Thajchayapong, M., Alibiglou, L., Lilaonitkul, T., & Mirbagheri, M. M. (2006). Mechanical abnormalities of the spastic ankle in chronic stroke subjects. [Research Support, U.S. Gov't, Non-P.H.S.]. *Conf Proc IEEE Eng Med Biol Soc, 1*, 3688-3691.

Twitchell, T. E. (1951). The restoration of motor function following hemiplegia in man. *Brain, 74*(4), 443-480.